



Publication Year	2020
Acceptance in OA	2021-01-19T12:48:51Z
Title	Search for the optical counterpart of the GW170814 gravitational wave event with the VLT Survey Telescope
Authors	GRADO, ANIELLO, CAPPELLARO, Enrico, Covino, S, GETMAN, FEDOR, Greco, G, Limatola, L, Yang, S, AMATI, LORENZO, BENETTI, Stefano, Branchesi, M, BROCATO, Enzo, BOTTICELLA, MARIA TERESA, Campana, S, CANTIELLO, Michele, DADINA, MAURO, D'AMMANDO, FILIPPO, DE CESARE, GIOVANNI, D'Elia, V, DELLA VALLE, Massimo, IODICE, ENRICHETTA, Longo, G, Mapelli, M, MASETTI, NICOLA, NICASTRO, LUCIANO, PALAZZI, ELIANA, POSSENTI, ANDREA, RADOVICH, MARIO, ROSSI, Andrea, SALVATERRA, Ruben, STELLA, Luigi, Stratta, G, TESTA, Vincenzo, TOMASELLA, Lina
Publisher's version (DOI)	10.1093/mnras/stz3536
Handle	http://hdl.handle.net/20.500.12386/29848
Journal	MONTHLY NOTICES OF THE ROYAL ASTRONOMICAL SOCIETY
Volume	492

Search for the optical counterpart of the GW170814 gravitational wave event with the VLT Survey Telescope

A. Grado^{1,2*}, E. Cappellaro³, S. Covino⁴, F. Getman¹, G. Greco⁵, L. Limatola¹, S. Yang³, L. Amati⁶, S. Benetti³, M. Branchesi^{7,8}, E. Brocato^{9,12}, M. Botticella¹, S. Campana⁴, M. Cantiello⁹, M. Dadina⁶, F. D’Ammando¹⁰, G. De Cesare⁶, V. D’Elia^{12,11}, M. Della Valle¹, E. Iodice¹, G. Longo¹³, M. Mapelli¹⁴, N. Masetti^{6,15}, L. Nicastro⁶, E. Palazzi⁶, A. Possenti¹⁶, M. Radovich³, A. Rossi^{6,11}, R. Salvaterra¹⁷, L. Stella¹², G. Stratta^{6,18}, V. Testa¹¹, L. Tomasella³,

¹ INAF, Osservatorio Astronomico di Capodimonte, Salita Moiariello 16, I-80131, Napoli, Italy

² INFN, - Sezione di Napoli - Complesso Universitario di M. S. Angelo, Ed. 6- Via Cintia, I-80126 Napoli, Italy

³ INAF, Osservatorio Astronomico di Padova, Vicolo dell’Osservatorio 5, I-35122 Padova, Italy

⁴ INAF, Osservatorio Astronomico di Brera, Via E. Bianchi 46, I-23807 Merate (LC), Italy

⁵ Università degli Studi di Urbino ‘Carlo Bo’, Dipartimento di Scienze Pure e Applicate, P.zza Repubblica 13, I-61029, Urbino, Italy

⁶ INAF - Osservatorio di Astrofisica e Scienza dello Spazio, Via Piero Gobetti 93/3, I-40129 Bologna, Italy

⁷ Gran Sasso Science Institute, Viale F. Crispi 7, I-67100 L’Aquila, Italy

⁸ INFN, Laboratori Nazionali del Gran Sasso, I-67100 Assergi, Italy

⁹ INAF, Osservatorio Astronomico d’Abruzzo, Via Mentore Maggini Teramo, TE, I-64100, Italy

¹⁰ INAF, Istituto di Radioastronomia, Via Piero Gobetti 101, I-40129 Bologna, Italy

¹¹ ASI Space Science Data Centre, Via del Politecnico snc, I-00133, Roma, Italy

¹² INAF, Osservatorio Astronomico di Roma, Via Frascati, 33, I-00040 Monte Porzio Catone, Roma, Italy

¹³ Università degli Studi di Napoli Federico II, Complesso Universitario di Monte Sant’Angelo, Via Cinthia, 21 Edificio 6, I-80126, Napoli, Italy

¹⁴ Physics and Astronomy Department “G. Galilei” University of Padova, Vicolo dell’Osservatorio 3 I-35122 Padova, Italy

¹⁵ Departamento de Ciencias Físicas, Universidad Andrés Bello, Fernandez Concha 700, Las Condes, Santiago, Chile

¹⁶ INAF, Osservatorio Astronomico di Cagliari, Via della Scienza 5, I-09047 Selargius (CA), Italy

¹⁷ INAF/IASF-MI, via Bassini 15, I-20133 Milano, Italy

¹⁸ INFN-Firenze, via Sansone 1, I-50019, Firenze, Italy

Accepted ... Received ...; in original form ...

ABSTRACT

We report on the search for the optical counterpart of the gravitational event GW170814, which was carried out with the VLT Survey Telescope (VST) by the GRAVitational Wave Inaf TeAm (GRAWITA). Observations started 17.5 hours after the LIGO/Virgo alert and we covered an area of 99 deg² that encloses $\sim 77\%$ and $\sim 59\%$ of the initial and refined localization probability regions, respectively. A total of six epochs were secured over nearly two months. The survey reached an average limiting magnitude of 22 AB mag in the r -band. After assuming the model described in Perna et al. (2019), that derives as possible optical counterpart of a BBH event a transient source declining in about one day, we have computed a survey efficiency of about 5%. This paper describes the VST observational strategy and the results obtained by our analysis pipelines developed to search for optical transients in multi-epoch images. We report the catalogue of the candidates with possible identifications based on light-curve fitting. We have identified two dozens of SNe, nine AGNs, one QSO. Nineteen transients characterized by a single detection were not classified. We have restricted our analysis only to the candidates that fall into the refined localization map. None out of 39 left candidates could be positively associated with GW170814. This result implies that the possible emission of optical radiation from a BBH merger had to be fainter than $r \sim 22$ ($L_{\text{optical}} \sim 1.4 \times 10^{42}$ erg/s) on a time interval ranging from a few hours up to two months after the GW event.

Key words: gravitational wave: general — gravitational wave: individual (GW170814); wide field surveys; VST

1 INTRODUCTION

August 14, 2017 is a milestone in the gravitational waves (GW) Astronomy. The Virgo interferometer (Acerese et al. 2015) detected its first signal and the triangulation with the LIGO interferometers (Aasi et al. 2015) led to a strong improvement of the sky localization of the event GW170814, shrinking the area of the original error box obtained by using only the LIGO detectors, from 1160 deg² to only 60 deg² after using all three detectors (Abbott et al. 2017a)¹. This was a fundamental step forward in the newly born era of multi-messenger astrophysics which was fully exploited three days later with the detection of the binary neutron stars merger GW 170817 event and its electromagnetic counterpart (Abbott et al. 2017b; Pian et al. 2017).

The GW170814 event was detected at 10:30:43 UTC; it is attributed to the merger of two black holes (BH) with a false-alarm rate of 1/27000 years. The estimated black hole masses are $30.5^{+5.7}_{-3.0} M_{\odot}$ and $25.3^{+2.8}_{-4.2} M_{\odot}$, while the inferred luminosity distance is 540^{+130}_{-210} Mpc² corresponding to a redshift $z = 0.11^{+0.03}_{-0.04}$ (Abbott et al. 2017a). In the O1 and O2 LIGO and Virgo observing run a total of 10 BBHs have been observed (The LIGO Scientific Collaboration et al. 2018b), allowing us to put constraints on a certain number of parameters associated to the population of BBHs. Among them it has been possible to infer a BBH merger rate density of ~ 60 Gpc⁻³yr⁻¹. Of high valuable scientific interest is their mass distribution, it comes out that there is a significant reduction in the merger rate for BBHs having primary masses larger than $\sim 45 M_{\odot}$, while the limited sensitivity does not allow to place reliable constraints on the minimum mass of black holes. The limited size sample and the local nature of the events so far observed have prevented to infer the BBH redshift distribution. A binary BH merging is not expected to produce an electromagnetic (EM) counterpart. However, there are alternative models (de Mink & King 2017; Perna et al. 2016, 2018; Zhang 2016; Murase et al. 2016; Yamazaki et al. 2016; Stone et al. 2017) which predict possible EM radiation in the optical/near infrared spectral region. If a fraction of the progenitors mass lost during the prior evolution of the binary stellar system, is retained as circumbinary disk, an infrared emission to medium-energy X-rays might be observable within hours after the GW event (de Mink & King 2017). In particular Perna et al. (2019) find that after one day from the GW event an optical signal in the R band could be detected at a magnitude of ~ 22.5 for a source at a distance of GW150914.

The detection of an EM counterpart of a GW emitted by a stellar BBH would reduce GW parameters degeneracy (see Pankow et al. (2017)), it would allow the measurement of the source redshift (Schutz 1986), and provide hints on the formation channel of the BBH binary by exploring the environment in which the merger occurred. Indeed dynamical formation (Rodriguez et al. 2016) is likely to take place in dense star clusters, while the isolated binary evolution is expected in typical field galaxies (Kalogera et al. 2007). The results of the search of optical counterpart to GW170814 event was recently published (Doctor et al. 2019). By using the Dark Energy Camera, 225 deg² were imaged corresponding to 90 per cent of the LALInference probable sky area. The observations have been

carried in the *i* band reaching a depth of ~ 23 mag. With a selection criteria optimized to search for fast declining (few days) transients two candidates were found. However, as stated by the authors, these candidates are most likely not associated with GW170814. This work is carried out within the GRAWITA collaboration (Brocato et al. 2018) and is organized as follows: section 2 describes the VST observational strategy, section 3 the processing of data and search for counterpart. In section 4 is described the survey detection efficiency calculation. Finally, we draw our conclusions in section 5.

2 VST OBSERVATIONAL STRATEGY

We carried out the search for the optical counterpart of the GW170814 event using the ESO VLT Survey Telescope (VST, Cappacioli et al. 2003) located at Cerro Paranal in Chile. VST is a 2.6m telescope specifically designed for wide-field imaging. It is equipped with OmegaCAM, a CCD mosaic camera made of 32 (2048 × 4096) pixel devices for a total 16k × 16k pixels, providing a field of view of ~ 1 deg² (Kuijken 2011). The standard filter set includes *ugriz* Sloan filters (Doi et al. 2010).

We started our observations 17.5 hours (Greco et al. 2017) after the LIGO/Virgo alert triggered by four independent low-latency pipelines at 2017-08-14 10:30:43 UTC (The LIGO Scientific Collaboration & the Virgo Collaboration 2017a). The sky area tiling was obtained using a dedicated tool named *GWsky*³. *GWsky* is a *python*⁴ tool developed to generate accurate sequences of pointings (tiles) covering the sky localization of a GW. It is equipped with a Graphical User Interface (GUI) optimized for fast and interactive telescope-pointing operations and supplies information and descriptive statistics on telescope visibility, GW localization probability, availability of reference images and coverage of catalogued galaxies for each FoV footprint. *GWsky* supports two observational strategies according to the preliminary information reported in the LIGO/Virgo GCN notices/circulars. They are (1) the tiling and (2) targeted searches. The tiling (or coverage) strategy mainly provides a list of pointings that (i) optimizes the telescope's visibility during the pre-assigned epochs, (ii) maximizes the contained localization probability and (iii) avoids areas with too bright objects and/or severe crowding. The second strategy generates a list of pointings covering galaxies from the Glade catalogue (Dálya et al. 2018) ranked from the highest to the lowest luminosity taking into account the initial airmass.

The posterior luminosity distance and standard deviation of GW170814⁵ were automatically taken from the FITS header of the initial BAYESTAR sky map (Singer & Price 2016) (DISTMEAN and DISTSTD) for rapidly setting an observational strategy. Given the nature of the event and its posterior mean distance, the number of galaxies contained in the sky error volume was found to be too high for a targeted search so that the *coverage* strategy was chosen. Starting from the maximum probability pixel of the BAYESTAR sky map, (RA[deg] = 41.06842, DEC[deg] = -45.48795) a sequence of 9 consecutive tiles (each tile is made of 3 × 3 pointings⁶) were defined limiting the airmass to 2 and maximizing the enclosed probability in each tile. The survey was performed in the *r*-band covering an

¹ The on-line False Alarm Rate (FAR) value is given in The LIGO Scientific Collaboration & the Virgo Collaboration (2019) and the final estimates of the parameters of the two black hole are given in The LIGO Scientific Collaboration et al. (2018a).

² We assume a flat cosmology with Hubble parameter $H_0 = 67.9$ km s⁻¹ Mpc⁻¹ and matter density parameter $\Omega_m = 0.3065$ (Planck Collaboration et al. 2016)

³ <https://github.com/ggreco77/GWsky>

⁴ <http://www.python.org>

⁵ The GW trigger was recorded with LIGO-Virgo ID G298048, by which it is referred throughout the GCN Circulars.

⁶ The choice of 3 × 3 *deg*² tiles is due to technical reasons, it optimizes the telescope overheads.

area of 81 deg^2 , enclosing the initial sky localization probability of ~ 76 per cent. The choice of the *r* band is a trade off between telescope and camera efficiency and expected spectral distribution of the electromagnetic signal.

On 2017 August 16, an updated localization from LIGO and Virgo data around the time of the compact binary coalescence was provided (The LIGO Scientific Collaboration & the Virgo Collaboration 2017b). Source parameters estimation were performed using the LALInference algorithm (Veitch et al. 2015) and a new sky map was available for retrieval from the GraceDB⁷ event page (hereafter, preliminary LALInference). The maximum probability pixel of the preliminary LALInference is localized at the coordinates RA[deg] = 46.53409, DEC[deg] = -44.59799. The 90 per cent credible regions of the initial (BAYESTAR) and his updated localization have significant overlap, but the 50 per cent credible region is shifted east by its entire width. To compensate such shift, 2 additional tiles were added (shown in light green in figure 1), for a total observed area of 99 deg^2 , starting from the third epoch enclosing a total probability of ~ 50 per cent of the Preliminary LALInference. On 2017 September 27, a refined sky localization was issued taking into account calibration and waveform modelling uncertainties (The LIGO Scientific Collaboration & the Virgo Collaboration 2017c).

The sky coordinates of the VST pointings and the enclosed probability for each tile are reported in Table 1. The enclosed probability is calculated with respect to the BAYESTAR (The LIGO Scientific Collaboration & the Virgo Collaboration 2017a), LALInference preliminary (The LIGO Scientific Collaboration & the Virgo Collaboration 2017b) and the final LALInference (hereafter, refined LALInference) skymaps. The refined LALInference was recently published in the Gravitational-Wave Transient Catalogue - GWTC-1 (The LIGO Scientific Collaboration et al. 2018a). The initial BAYESTAR sky localization and the refined LALInference sky localization, as well as the VST tiles, are shown in Fig. 1. We covered a total area of 99 deg^2 , taking into account uncovered gaps among ccds, haloes and spikes due to bright stars, we encloses ~ 77 per cent and ~ 59 per cent of the initial and refined localization probability region, respectively.

The VST observations are organized in observing blocks (OB) consisting of a mosaic of 9 pointings – $1 \times 1 \text{ deg}^2$ – hence covering a total area of $3 \times 3 \text{ deg}^2$. Each pointing is made of two exposures of 40 s each dithered by $0.7 - 1.4$ arcmin. The dithering allows us to fill the gaps in the OmegaCAM CCD mosaic. The VST observations of the patrolled area were repeated six times distributed over \sim two months in order to have enough data points to sample the light curve of the optical transients. A 50% point sources completeness at $r \approx 22.0$ AB mag was reached in most epochs.

A summary of the VST observations performed for the GW170814 event is reported in Table 2. In some epoch it was not possible to cover the whole area in one single night. In Tab. 2 we also report the average seeing (FWHM), the minimum and maximum values of the airmass, the magnitude corresponding to 50% completeness and the minimum and maximum value for the different pointings⁸. An overview of the temporal distribution of the observations along with the observing conditions is shown in Fig. 2.

⁷ <https://gracedb.ligo.org/>

⁸ The 50% completeness is estimated using *VST-Lim*, a tool of the VST-Tube pipeline (Grado et al. 2012), that adds to the image under analysis simulated point sources (generated using Skymaker, Bertin 2009) and counts for the number of recovered sources as function of the magnitude.

3 DATA PROCESSING

3.1 Pre-reduction

Immediately after acquisition, the images were mirrored to the ESO Garching data archive, and then transferred by an automatic procedure from the ESO Headquarters to the VST Data Center in Naples (Italy). The first part of the image processing was carried out using *VST-tube* (Grado et al. 2012), which is a data reduction pipeline specifically developed for the VST-OmegaCAM mosaics. It performs pre-reduction, astrometric and photometric calibration and mosaic production.

To remove the instrumental signatures, after overscan, bias and flat-field corrections, we performed gain equalization of the 32 CCDs and illumination correction. The last step was achieved by comparing the magnitude of stars with the SDSS DR12 catalogue (Alam et al. 2015) in equatorial fields observed during the same nights. The magnitude difference as function of the position over the whole field of view is fitted using the “generalized additive method” (Hastie & Tibshirani 1986). This approach has been shown to be more robust compared to a plain surface polynomial fit in particular for what concerns the behavior at the edges of the image. Then, the position-dependent zero-point correction was applied to science images. The relative photometric calibration of the images was obtained by minimizing the quadratic sum of differences in magnitude between sources in overlapping observations. The tool used for both the astrometric and relative photometric calibration tasks is SCAMP (Bertin 2006). The used reference astrometric catalogue is 2MASS (Skrutskie et al. 2006). The absolute photometric calibration was obtained with the Photcal tool (Radovich et al. 2004) using as reference the equatorial photometric standard star fields from SDSS DR12 (Alam et al. 2015). Finally the two dithered images for each pointing were co-added. In order to simplify the subsequent image subtraction analysis, for each pointing the mosaics at the different epochs were registered and aligned to the same pixel grid. This assures that each pixel in the mosaic frame corresponds to the same sky coordinates for all epochs. For further details on the data reduction see Capaccioli et al. (2015).

The detection of transients is affected by the presence of artifacts on the images. These artifacts can be due to the telescope, like spikes and haloes around bright stars, and/or to the camera, like electronic cross-talk. It is desirable to detect and correct them or at least to identify the pixels affected by the artifact. With this purpose we produce a flag image with specific code for different kind of contaminants that can be used during image analysis. The procedure to mask the spikes around bright stars is described in appendix A whereas in the following we describe the approach adopted for cross talk. In fact, two CCDs of the OMEGACAM camera (ccd65 and ccd66 in ESO names coding; c.f. (Mieske 2018)) are affected by electronic cross-talk, i.e. the appearing of spurious sources or holes due to the presence of bright sources in the corresponding pixels of the other CCDs. This produces spurious sources that can be confused with transients. In principle with the knowledge of the cross-talk coefficients one can attempt to remove the ghost objects. In practice the coefficients change with time then preventing a safe removal of the spurious sources. For that reason we decided to adopt a conservative approach masking the pixels affected by cross-talk ghosts with a specific flag value.

With the current available hardware, the time needed to produce a one square degree fully calibrated co-added image is ~ 20 min, including the time for data transfer from Cerro Paranal to Naples and the production of the *SExtractor* catalogues.

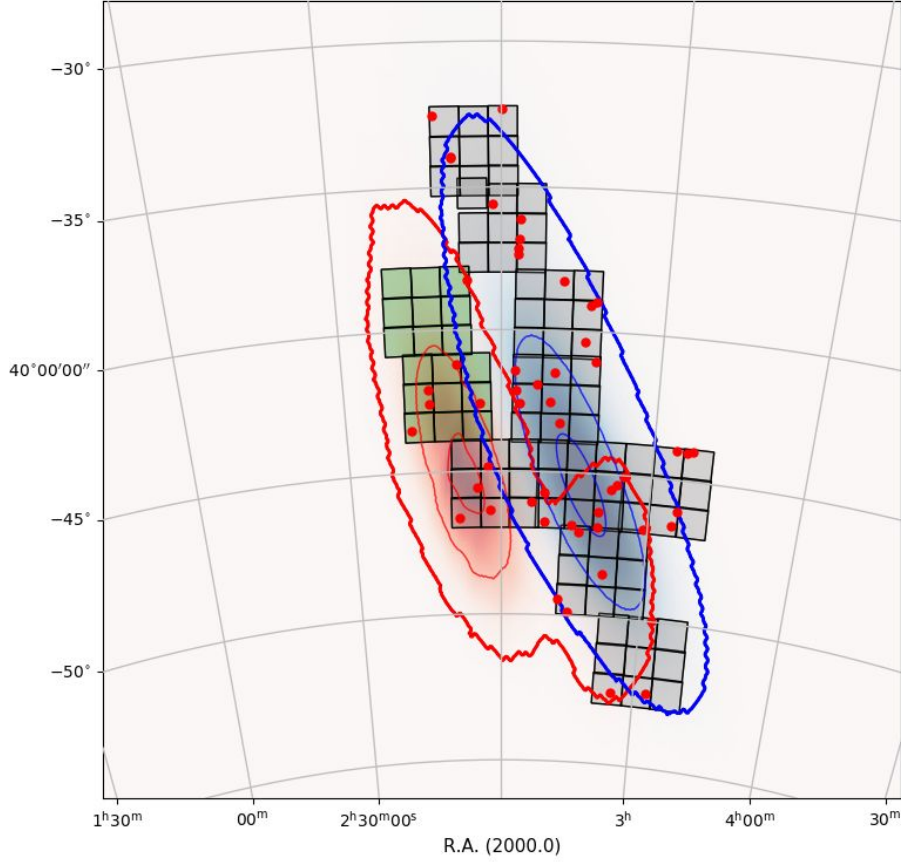


Figure 1. Footprints of the VST r -band observations over the contours of both the initially distributed BAYESTAR and refined LALInference sky localization maps of GW 170814. Each small square represents a VST observation. The blue and red external contours are the initial localization and refined map at 90 per cent confidence level, respectively. The inner contour lines represent the enclosed probabilities of 50 per cent and 10 per cent confidence level, respectively. The tiles in light green are observed since the third epoch.

Table 1. Summary of the VST tiled observations. For each pointing the contained probability is measured from the initial to the final GW170814 sky localization. The last two tiles T_{10} and T_{11} were observed starting from the third epoch.

Tile	RA ICRSd	Dec ICRSd	BAYESTAR Contained Probability (%)	Preliminary LALInf. Contained Probability (%)	Refined LALInf. Contained Probability (%)
T_1	02:44:16.421	-45:29:16.62	22.0	2.3	1.9
T_2	02:27:09.286	-45:29:16.62	3.8	0.6	0.7
T_3	03:01:23.556	-45:29:16.62	2.6	15.0	22.0
T_4	02:49:41.880	-42:29:16.62	17.0	1.5	0.5
T_5	02:49:41.880	-39:29:16.62	7.1	0.4	0.08
T_6	02:38:50.962	-48:29:16.62	14.0	3.1	4.1
T_7	02:59:53.815	-36:29:16.62	3.7	0.5	0.1
T_8	03:04:41.582	-33:48:16.60	1.5	0.4	0.07
T_9	02:29:17.376	-51:29:16.62	3.8	1.7	1.8
T_{10}	03:10:23.030	-42:25:52.18	0.7	14.0	20.0
T_{11}	03:13:39.854	-39:22:22.33	0.6	10.0	7.8

3.2 Transient search

In order to search for variable and transient sources, we applied our analysis procedure first described in Brocato et al. (2018). The pipeline is based on two independent yet synergistic procedures.

One, called *ph-pipe*, is based on the comparison of the photometric measurements of all the sources in the VST field obtained at different epochs. The second (*diff-pipe*) is based on the analysis of the difference of images following the approach of the supernova

Table 2. Summary of the VST observations performed for the GW170814 event. One epoch is completed when the whole sky map is covered. For observational constraints not necessarily one epoch is completed in a single night as reported in column 1. The second column reports the night that includes all the observations carried out between 12:00 UT of the indicated night and finished at 12:00 UT of the day after. The third column reports the covered area in deg^2 . Then, it is shown the average FWHM, the minimum and maximum values of the airmass, the average 50 per cent completeness limit and its min and max values.

Epoch	Date (UT)	Area deg^2	FWHM arcsec	AIRMASS min-max	compl. avg 50%	compl. min-max
1	2017-08-14	81	1.04	1.05-1.98	22.0	21.8-22.3
2	2017-08-16	81	1.23	1.05-1.98	22.0	21.4-22.4
3	2017-08-18	45	1.29	1.15-1.98	21.8	21.2-22.3
3	2017-08-19	45	1.31	1.05-1.79	22.0	21.6-22.4
4	2017-08-24	38	1.39	1.08-1.79	21.9	21.6-22.2
4	2017-08-26	31	1.12	1.05-1.98	22.2	22.0-22.4
4	2017-08-27	9	1.03	1.39-1.51	22.4	22.5-22.5
5	2017-09-11	36	1.46	1.08-1.25	21.5	21.2-21.9
5	2017-09-12	43	1.52	1.05-1.98	21.7	21.5-22.1
5	2017-09-14	18	1.07	1.22-1.51	22.2	22.1-22.4
6	2017-09-27	63	1.19	1.05-1.79	22.0	21.5-22.4
6	2017-09-28	36	0.72	1.22-1.98	22.0	21.6-22.3

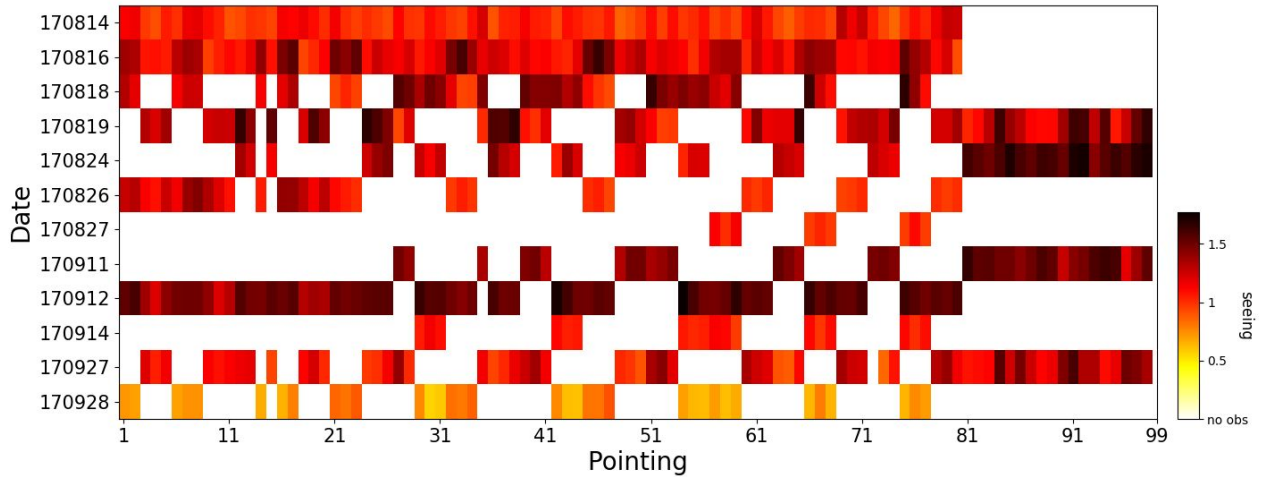


Figure 2. Overview of the survey monitoring progress. On ordinates are indicated months and days. On abscissa the VST pointings of $1 \times 1 \text{ deg}^2$. The color indicates the seeing achieved for each specific pointing. Please refer to Table 2 to see the way nights are grouped for each epoch.

(SN) search program conducted with the VST for several years now (Cappellaro et al. 2015).

The *ph-pipe* is typically more rapid, providing an excellent quick-look facility able to single out candidates in single epoch campaigns

while the *diff-pipe* is more effective for pinpointing sources projected over extended objects or in case of strong crowding. The two approaches are complementary and since they are independent the comparison of the results allow us to spot possible missed transients.

As discussed in Brocato et al. (2018) the list of candidates contains a large number of spurious objects that can be related to small misalignments of the images, improper flux scaling, incorrect PSF convolution or *not* well masked CCD defects and cosmic rays. In most cases spurious transients could be easily identified by visual inspection. However due to the large number of candidates it would be very time consuming. For this reason both pipelines apply several

criteria to attribute a “score” to select “bona fide” candidates, based on their morphological parameters, magnitude variations, positions with respect to nearby galaxies, etc. (c.f. Cappellaro et al. 2015). With this approach we can readily reject most spurious sources. The remaining candidates go through a further selection after being visually inspected.

In consideration of the largely unknown properties of the possible EM gravitational wave counterpart, we decided not to use model-based priors in the candidate selection. The main goal of our analysis is therefore to simply identify sources showing a “significant” brightness variation (5σ between at least two epochs that in our case corresponds typically to ~ 0.5 magnitudes), either rising or declining in flux during the monitoring.

The implementation of the *diff-pipe* requires adequate reference images. Ideally, these images should be obtained before the event to allow for a prompt transient search. If they are not available, as it is in our case, they can be obtained at later epochs. Alterna-

Table 3. Scoring conditions

condition	score	number
FWHM/avg(FWHM) > 2.5	-60	1,415,908
ISOAREA < 2×avg(FWHM)	-60	475,738
$N_{\text{pix}}(\text{positive})/N_{\text{pix}}(\text{Negative}) < 0.60$	-60	3,435,173
remaining with score > 0		133,956
2.5 > FWHM/avg(FWHM) > 1.75	-30	62,712
$2 \times \text{avg}(\text{FWHM}) < \text{ISOAREA} < 3 \times \text{avg}(\text{FWHM})$	-30	38,138
$N_{\text{pix}}(\text{positive})/N_{\text{pix}}(\text{Negative}) < 0.70$	-30	68,295
near star mag < 17	-30	45,215
near galaxy	+30	6519
remaining with score > 0		10714

tively, we can use as references archival images obtained with other telescopes. Archival images of the survey area of GW170814 are available from the DECAM survey archive⁹. This option is not immune to risk due to a possible mismatch of the instrument/telescope band-passes, objects with a peculiar spectrum give rise to spurious transients after image subtraction (notice however that such objects will give a constant residual for all the different VST epochs).

Conservatively, in the case of GW170814 we performed the transient search using as reference the VST late time images whereas DECAM reference images were used to produce the transient light curves (cf. later this section). This was also useful to verify the possible use of archive DECAM images for future prompt searches.

The difference images produced with *hotpants* for the 99 pointings were searched with *SExtractor* resulting in a cumulative list of 3,974,951 variable sources. The list is large because we adopted a low detection threshold (1.5σ above the background noise) to make sure to get the faintest transients. This also means that most of the detected sources are spurious due to noise fluctuation, image defects, not well removed cosmic rays or imperfect subtraction of bright stars, etc. Following *Cappellaro et al. (2015)* to filter out most of the spurious candidates we used a scoring algorithm based on several metrics of the detected candidates following the scheme reported in Tab. 3.

The numbers in Tab 3 includes multiple detections at different *epochs*. In fact, the final list with score > 0 counts 9,342 distinct candidates of which 1,687 with high score (≥ 60). The first condition in Tab 3 adds a penalty of 60 to objects that appear to be non stellar in the difference image. The second condition helps to remove cosmics that were not detected in the early stages of the image processing. The third condition gives a strong penalty to those sources caused by a local mismatch of the PSF that usually gives a "dipolar" source with positive and negative pixels counts. Then the scoring is repeated with more stringent parameters but with less heavy penalties. *Ratings are applied in order to penalise spurious detections with the exceptions of "near galaxy sources", a condition that raises the rank of these objects to a positive score.*

The scoring algorithm and reference value were chosen after extensive artificial star experiments. We found that with the above scoring scheme and selecting a score threshold > 0 we can reject > 99% of spurious candidates at the cost of losing 5% of the real transients. After adopting a score threshold of 60% the number of

spurious events decreases by a factor ~ 5 whereas the fraction of real transients that are lost may increase up to by 15%.

In this work we visually inspected all candidates with score > 0 which led to a list of 246 validated transients.

We cross-checked the candidates with public data-sets, e.g. SIMBAD (*Wenger et al. 2000*), NED¹⁰, and Skybot (*Berthier et al. 2006*), aiming at identifying known objects. This allowed us to remove from the list two RR Lyrae, and 21 asteroids. We also removed transients that are bona fide variable stars because they coincides with stellar sources present in all our images and also in the DECAM archive images.

We are left with a total number of 53 candidates (36 were identified by both pipelines and 17 only by *diff-pipe*), see Appendix B.

Since all the selected candidates are also located in the survey area of the Dark Energy Survey, we took DES images observed before the GW event as reference frames to investigate the sources variability. Details of the 53 candidates transients, namely their photometric catalogue and light curve analysis, are reported in Table B1 and 4. We have differentiate the transients found by both the search pipelines (the prefix *c* in the Id) from the ones found only with the image subtraction pipeline (prefix *d* in the Id). We reported whether a source was found in the NED (within 5 arcsec) or SIMBAD (within 3 arcsec) (column 4 and 5 of table 4, respectively) and the identification that comes from these databases. In figure 3 we show the light curves for all 53 candidates. In case of missing detection it is reported the limiting magnitude of the image at the specific epoch.

For transients with only one detection we can exclude that they are normal SNe (of any kind) or AGN (they are not associated with galaxy nuclei). We cannot exclude unknown asteroids, peculiar fast transients, flare stars (even if they are much rarer). When multiple detections for a given transient were available we attempted to perform a transient classification using the approach described in Sect. 4 of *Cappellaro et al. (2015)*. In short, the transient light curve was compared with that of templates SNe of different types assuming as a free parameters the phase and redshift. In practice, for each template we compute a grid of simulated light curves in a range of redshift by applying the appropriate k-correction and time dilation. The best fit is chosen by chi-square minimization (due to the lack of color information we cannot constrain the extinction that is neglected). In this approach, the shape of the light curve is the main constraint for the template selection while the apparent/absolute magnitude comparison set the redshift for the specific template. In fact, only in two cases the redshift of the host was known from NED. Yet, because of the very sparse light curve sampling, limited number of epochs and lack of color information no firm classification could be secured. We could only conclude that two dozen transients have the light curve consistent with that of a specific SN type at a given redshift (and are then considered SN candidates). In addition, ten events are identified as AGN candidates because they are hosted in galaxy nucleus and shows erratic variability. *Finally, for nineteen transients, with only one detection no specific class could be assigned.*

One of the candidate AGN is indeed classified as a QSO in the NED database. Also, three of the SNe candidate are listed in the Transient Name Server (TNS)¹¹ as follows:

- the transient d3 of table B1 has a light curve shown in Fig. 4

⁹ <http://archive.noao.edu>

¹⁰ <https://ned.ipac.caltech.edu/>

¹¹ <https://wis-tns.weizmann.ac.il/>

Table 4. Results from the transient search and identification. In the ID column c indicates that the object was found in both diff-pipe and ph-pipe pipelines, d that the transient was found only with the image subtraction pipeline. In columns 2 and 3 we list RA and DEC (J2000); column 4 and 5 reports if the source was already present

in NED and SIMBAD database respectively. Column 6, 7 and 8 report average magnitude, magnitude variance and number of available magnitudes including upper limits where available. Column 9 reports the template used and the results of the light curve fit, where z is the best-fit redshift, p is the phase. Column 10 lists the probability at the position in the LALInference map for each candidate. The map has been divided in bins of 10% of integrated probability, the reported number is the upper limit of the bin. For example the candidate d9 is at a position located in the region of the sky map enclosed between 80 and 90% of confidence levels. After 90 % we added two further bins: 90-95% and 95-99%. Candidates with values 99 are outside the sky map region for that reason unrelated to the GW event. In the last column, where applicable, are noted remarks about the identification.

Id	RA	Dec	NED	SIMBAD	mag_{mean}	mag_{var}	N_{mag}	light curve fit	Localization	Note
c1	47.93876	-32.50572	-	-	20.64	>2.8	1	-	99	1
c2	41.12476	-47.08170	-	-	20.36	0.38	4	Ia 1990N $z=0.12$ $p=8$	80	
c3	44.24308	-36.10156	-	-	19.82	>3.1	1	-	99	1
c4	43.55516	-46.05383	-	-	20.98	>2.9	1	AGN	80	
c5	39.56146	-45.53453	-	-	20.45	0.11	2	IIP 1999em $z=0.04$ $p=15$	80	
c6	44.29046	-37.11974	-	-	19.72	1.08	4	Ia faint 1991bg $z=0.06$ $p=5$	99	
c7	36.37832	-46.60462	Y	-	18.85	>3.5	1	-	95	1
c8	35.69231	-43.94526	-	-	20.39	0.17	2	Ia 1994D $z=0.05$ $p=42$	99	
c9	40.96637	-39.09182	-	-	19.15	>2.4	1	-	99	1
c10	42.84391	-46.75855	Y	-	19.70	1.41	6	IcBL 1998bw $z=0.09$ $p=0$	80	
c11	47.22520	-33.98899	Y	-	20.34	1.98	3	Iapcc 2000cx $z=0.08$ $p=20$	95	
c12	48.52714	-42.08370	-	-	19.85	0.47	2	1990N $z=0.07$ $p=0$	30	
c13	40.71350	-38.97058	-	-	19.25	>3.7	1	-	99	1
c14	36.19326	-46.11161	-	-	20.11	>2.3	1	-	95	1
c15	49.44558	-43.49652	-	-	19.41	>3.4	1	-	60	1
c16	43.33967	-41.94081	-	-	19.25	>3.6	1	-	95	1
c17	42.54444	-41.49203	-	-	20.34	>2.7	1	-	95	1
c18	47.20362	-41.20692	Y	-	20.91	>0.6	1	AGN	50	
c19	42.06331	-49.45406	-	-	20.14	>2.9	1	-	80	1
c20	36.50260	-43.98644	-	-	21.02	2.05	6	Ia 1992A $z=0.07$ $p=-25$	95	
c21	41.17931	-40.37404	Y	-	19.04	1.13	6	Ia 2002bo $z=0.055$ $p=-10$	95	
c22	36.94201	-49.98622	-	-	20.59	>2.1	1	-	80	1
c23	42.92521	-45.71532	-	-	21.27	>1.0	1	-	80	1
c24	42.71470	-42.51475	-	-	20.16	>3.8	1	-	95	1
c25	40.17324	-46.87562	-	-	20.27	>2.9	1	-	70	1
c26	42.22224	-38.25838	-	-	21.19	2.83	3	Ia 1990N $z=0.1$ $p=22$	99	
c27	40.63033	-41.06565	Y	-	21.05	1.37	7	Ia 1994D $z=0.071$ $p=0$	95	2
c28	36.88136	-52.49284	-	-	20.25	0.69	2	Ia 1990N $z=0.095$ $p=41$	90	
c29	48.50660	-42.58589	-	-	20.29	>3.2	1	-	30	1
c30	35.93385	-44.02682	Y	-	19.52	1.64	3	SNLC 2008es $z=0.14$ $p=21$	99	
c31	47.23585	-46.62792	-	-	19.30	0.80	3	Ia 1992A $z=0.05$ $p=35$	20	
c32	46.59110	-38.23088	-	-	19.77	2.96	3	Ia 1994D $z=0.05$ $p=20$	90	3
c33	46.09634	-42.57915	-	-	20.42	>1.9	1	-	50	1
c34	38.97934	-45.03692	-	-	20.81	1.24	2	-	80	1
c35	38.86904	-52.55772	-	-	19.99	3.66	3	-	80	1
c36	39.28249	-45.36645	-	-	20.05	>2.9	1	-	80	1
d1	42.24100	-43.27893	Y	-	20.60	3.04	7	Ia 1992A $z=0.12$ $p=-6$	95	
d2	44.27798	-36.80744	Y	-	20.45	0.56	6	IIP 1999em $z=0.04$ $p=0$	99	
d3	46.29475	-45.55090	Y	Galaxy	17.76	0.90	7	SLSN 2008es $z=0.0815$ $p=5$	99	4
d4	44.32350	-37.35107	Y	-	19.58	0.72	6	AGN	99	
d5	41.50049	-46.85482	Y	QSO	17.44	0.36	6	AGN (1.385)	80	5
d6	45.05304	-32.30412	-	-	18.80	0.77	6	AGN	99	
d7	37.81450	-46.85080	Y	-	19.57	2.30	6	Ia 1991bg $z=0.05$ $p=6$	80	
d8	40.11296	-46.33456	-	-	20.52	1.06	6	Ic 2007gr $z=0.07$ $p=0$	80	
d9	44.17079	-42.58189	-	-	20.28	1.19	7	Ia 1992A $z=0.08$ $p=2$	90	6
d10	41.56164	-49.89749	Y	AGN	18.83	0.77	6	AGN	80	
d11	47.19114	-33.94179	Y	-	19.52	0.80	6	AGN	95	
d12	39.78474	-48.51388	Y	-	18.96	0.44	6	Ia 1994D $z=0.095$ $p=0$	70	
d13	45.63721	-46.35241	-	-	20.23	0.91	7	Ia faint 1991bg $z=0.08$ $p=2$	10	
d14	45.75856	-44.83118	Y	-	20.16	1.24	6	Ia 1990N $z=0.1$ $p=40$	20	
d15	44.42912	-41.44589	Y	-	19.85	1.41	7	AGN	90	
d16	44.37912	-42.12675	Y	-	19.50	1.83	7	AGN	90	
d17	45.45381	-35.57484	-	-	20.36	0.60	6	AGN	99	

Notes 1 - Peculiar transient or unknown asteroid or possible flare star; 2 - host galaxy redshift from NED; 3 - AT 2017gqz in the Transient Name Server (TNS); 4 - host galaxy redshift from NED, SN2017eni in TNS; 5 - redshift from NED; 6 - AT 2017fat in TNS.

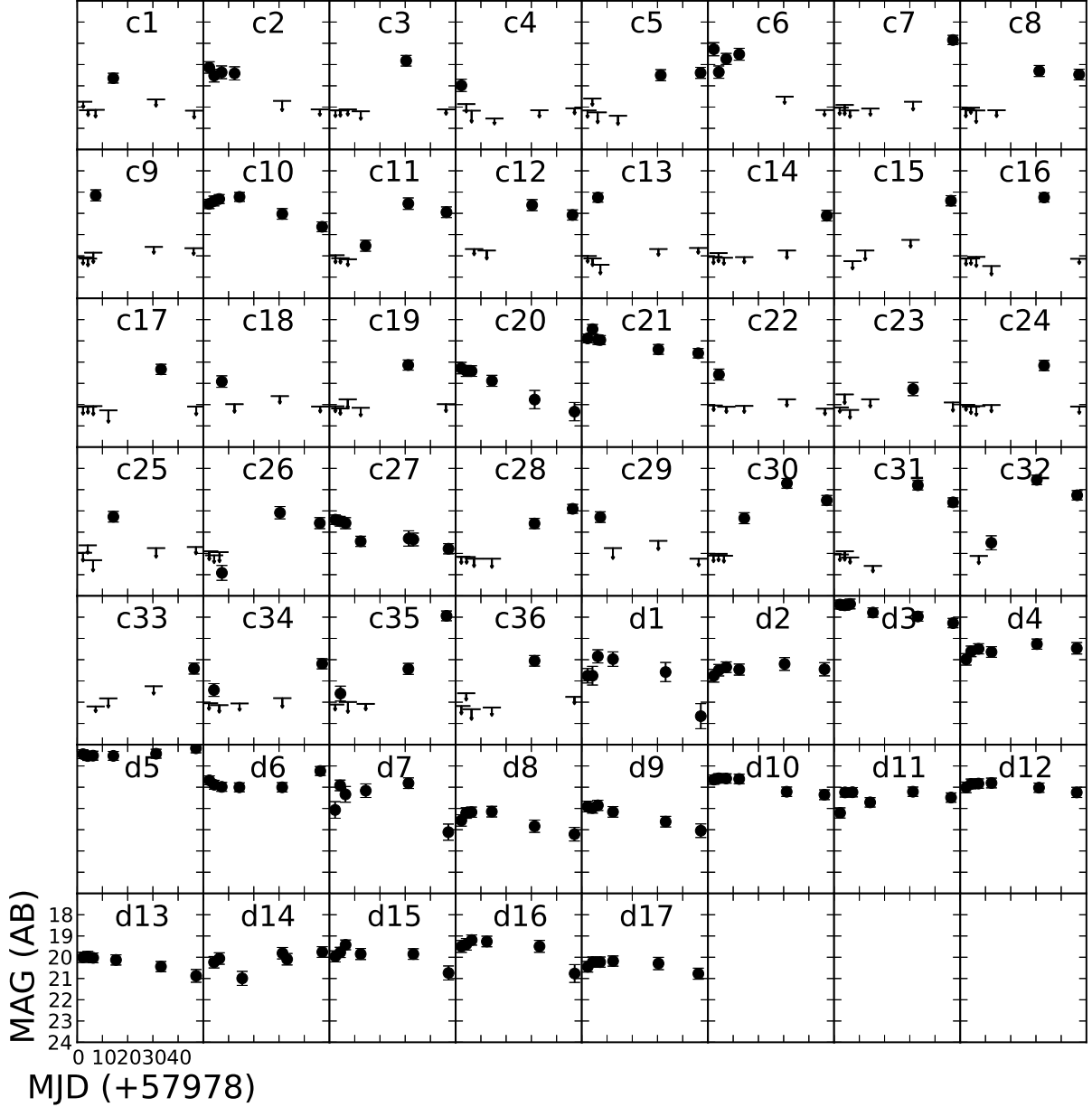


Figure 3. The light curves of the transient candidates found with the VST in 99 deg^2 covering the GW170814 error area. Arrows indicate the upper limit magnitude for the undetected sources.

top panel and was obtained by diff-pipe. By assuming the known redshift $z=0.0815$ (Miller et al. 2009), we identified it as a super luminous type II SNe similar to SN 2008es.

Indeed we found that the candidate d3 is coincident with SN2017eni (Gaia17blw). This was announced by Gaia Alerts (Delgado et al. 2017) on 2017 June 6 with $G=17.7$ mag and indicated as a SN candidate in the galaxy 6dFGS gJ030511.0-453304. It was

spectroscopically classified as a Type II_n superluminous supernova by Strader et al. (2017). Photometry from the ASAS-SN survey finds a peak at $V=16.9$ mag on 2017 Jun 6.44, implying an absolute magnitude of $M_V = -21.0$ mag.

- Transient c32 is coincident with AT 2017gqz (Gaia17cgz) announced as a Gaia transient on 2017-09-08 17:47:02 with $G=18.79$

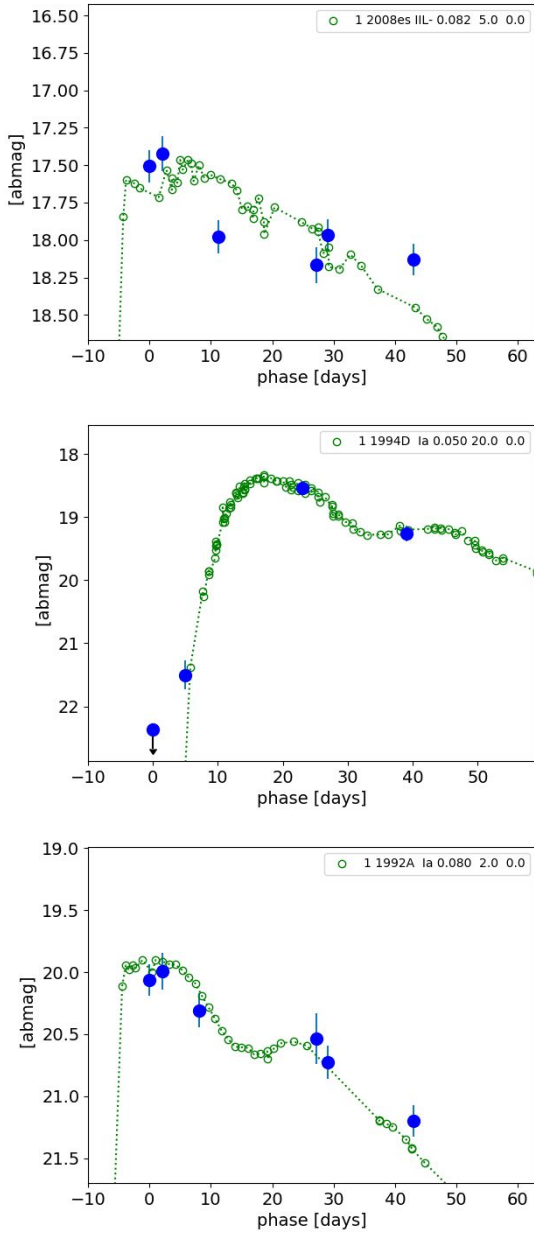


Figure 4. Top panel: best fit for transient d3 (SN2017eni, blue points) with the template SLSN 2008es (green dots). Mid panel: best fit for transient c32 (AT 2017gqz, blue points) and the SN Ia 1994D (green dots). Bottom panel: best fit for transient d9 (AT 2017fat, blue points) and the SN Ia 1994D (green dots). In the upper right boxes are reported the template used, the redshift and the phase. The last values, always equal to zero, are the extinction.

mag. Our light curve fitting shows that the transient is consistent with a type Ia SN at redshift 0.05 (see Fig. 4 mid panel).

- Transient d9 is coincident with AT 2017fat (Gaia17bqm) announced as a Gaia transient on 2017-06-05 00:41:45 with $G=18.18$ mag. The light curve fitting is consistent with that of a Ia SN at a redshift 0.08 (see Fig. 4 bottom panel).

We compared our search with the work carried out by Doctor et al. (2019). The Table 5 summarize the comparison of the two follow-up programs in terms of area covered, filter used, depth,

number of epochs, time span of the search, total uncertainty enclosed by the surveyed area.

In Doctor et al. (2019) two candidates with coordinates 1) RA= 42.35047 DEC=-40.32632 and 2) RA=47.63365 and DEC=-36.36045 were found. The second object is outside our searching region while in the position of the first one we have detected a source at magnitude between 22.5 and 23.5 (as reported by Doctor et al. (2019)), which is too faint to be qualified as a transient in our catalogue.

4 DETECTION EFFICIENCY

To evaluate the survey efficiency we need to know the expected optical light curve of the transient following a BBH merger. The latter is very uncertain although most authors agree that the optical emission should be expected much fainter and more rapid declining than the kilonova following a BNS merger. To explore the performance of our search we use as reference the most recent models of Perna et al. (2019) that likely encompass the range of possible electromagnetic transient from BBH merger. The different prediction are characterized by: a) jet energy in the range $10^{46} - 10^{49}$ erg; b) jet opening angle in the range 10-40 deg; c) jet Lorentz factor Γ (10 or 100). All models are computed for an ambient number density 0.01 cm^{-3} . We immediately verify that a large class of the Perna et al. (2019) models predict optical transients that, for the given distance of GW170814, are too faint for our instrumentation. In particular all models with energy $\leq 10^{47}$ erg are too faint regardless of the Γ factor and jet opening angle.

We are just marginally sensitive to models with energy 10^{48} erg only if the jet opening angle is small and our line of sight is along the jet. In the more favorable case of high Γ factor, the transient remain above mag 22 for about one day.

We have a measurable efficiency only for 10^{49} erg events characterized by high Γ factors.

To estimate the chance of detection of a possible optical transient after BBH we used the simulation of Perna et al. (2019), as follows.

For each model:

- 1 - we compute the predicted light curve in apparent magnitude at the distance of the transient (540 Mpc) for all the different viewing angles;

- 2 - for each pointing and epoch we verify whether the predicted magnitude is brighter that the magnitude limit.

- 3 - by considering the probability area covered by the specific transient and the solid angle fraction covered by the viewing solid angle, we compute the chance of detection for the specific pointing.

- 4- the chance of detection for the full survey is obtained by summing the probability for all pointings. In the best case of $\Gamma = 100$ and jet energy 10^{49} erg, with a view angle of 40 deg we obtain a survey efficiency of 5.1 per cent.

A more accurate estimation of the survey efficiency would require a Monte Carlo simulation where synthetic sources extracted from a population following the Perna et al. (2019) models are added to the images. Then the pipeline procedure to detect the transients is applied to recover the simulated sources. Considering the low efficiency, even for the best case, this procedure would not change significantly the results.

Table 5. Summary of the comparison between VST and DECam observations. For this work the area coverage reported in the table is the maximum area covered in one of the epochs observed (due to telescope operation constraints not always the whole area was covered). The depth for VST is the 50 % completeness limit for point like sources while in Doctor et al. is reported the 5σ magnitude limit for point-like sources. The total uncertainty covered refers to the refined localization probability region.

Survey	Area coverage (deg ²)	filters	depth	number of epochs	time span (days)	total uncertainty covered (%)
This work	up to 117	r	22	6	45	59
Doctor et al.	225	i	23	8	12	90

5 DISCUSSION AND CONCLUSIONS

We reported on the search for the optical counterpart for the GW event GW170814, by exploiting the capabilities of the VLT Survey Telescope. We covered a search area up to 99 deg², corresponding to 59 per cent of the credible region, repeated in six epochs distributed over ~ 2 months. A 50 per cent point source completeness at $r \simeq 22$ AB mag was reached in most of the epochs. This threshold corresponds to a luminosity limit of $L_{\text{optical}} \sim 1.4_{-1}^{+0.7}$ in unit of 10^{42} erg/s after assuming a light flat spectrum and a GW170814 median distance. The errors on the luminosity mostly derive from the uncertainty on the GW source distance. To estimate the survey efficiency we have considered the recent model for electromagnetic counterpart from binary black holes mergers described in Perna et al. (2019). In the most favorable case of a very energetic jet emission (10^{49} erg) and high Γ factor the expected magnitude of the transient source, at the distance of GW170814, is estimated to remain brighter than mag 22 for about a day. Therefore, under these specific conditions the corresponding survey efficiency is considerably low, about 5%. For optical transients search we developed a pipeline based on two independent analysis algorithms, one based on source extraction and magnitudes comparison between different epochs and the other based on transient identification obtained through image subtraction techniques. We present the catalogue of these transients, including, when possible, matches with the SIMBAD within 2 arcsec or NED catalogues and/or possible identification based on light-curve fitting. We identified two dozen candidates SNe, nine AGN candidates, one QSO. Nineteen transients have not been previously catalogued and since they have only one detection cannot be classified. For the sake of completeness we have reported in the paper all (53) candidates found. However, if we consider only the ones that fall into the refined localization map, the number decreases to 40. After removing d9, which was identified as a GAIA transient before the occurrence of the GW event, we are left with 39 "bona fide" candidates.

Our first two runs were carried out within two days from the gravitational wave event then the observations became more sparse (this also because we prioritize observations of the kilonova AT 2017gfo). It is worth noting that the tiles added to improve the coverage of the refined map started from the third epoch and that they cover almost half of the total contained probability. This implies that our observations tend to constrain models that predict slow-declining light curves like in Bartos (2016); Stone et al. (2017) where a new BBH formation channel inside AGN discs is proposed. In these models the presence of substantial gas densities around the merging stellar mass BHs can produce strong, slow-transient EM counterpart. In this respect our work is complementary to the work of Doctor et al. (2019) that put constraints on fast fading transients.

Particularly one of the two candidates that they found is outside our search area and the other one is too faint

The VST plan for future electromagnetic follow-up of BBH mergers is to have two or more observing epochs within the first couple of days after the alert to search for fast-declining transients and then keep observing for few weeks to put constraints on those models that predict slower declining light curves.

ACKNOWLEDGEMENTS

The authors thank the anonymous reviewer for constructive comments on the manuscript. This paper is based on observations made with the ESO/VST. We acknowledge the usage of the OmegaCam and VST Italian GTO time. We also acknowledge INAF financial support of the project "Gravitational Wave Astronomy with the first detections of adLIGO and adVIRGO experiments". This research has made use of public data of the LIGO Scientific Collaboration and the Virgo Collaboration. LIGO is funded by the U.S. National Science Foundation. Virgo is funded by the French Centre National de Recherche Scientifique (CNRS), the Italian Istituto Nazionale della Fisica Nucleare (INFN) and the Dutch Nikhef, with contributions by Polish and Hungarian institutes. S. Covino acknowledges partial funding from Agenzia Spaziale Italiana-Istituto Nazionale di Astrofisica grant I/004/11/3. A. Rossi acknowledges support from Premiale LBT 2013. We acknowledge partial support by the PRIN-INAF 2016 with the project "Towards the SKA and CTA era: discovery, localisation, and physics of transient sources" (P.I. M. Giroletti). This project used public archival data from the Dark Energy Survey (DES) as distributed by the Science Data Archive at NOAO. Funding for the DES Projects has been provided by the DOE and NSF (USA), MISE (Spain), STFC (UK), HEFCE (UK), NCSA (UIUC), KICP (U. Chicago), CCAPP (Ohio State), MIFPA (Texas A&M), CNPQ, FAPERJ, FINEP (Brazil), MINECO (Spain), DFG (Germany) and the collaborating institutions in the Dark Energy Survey, which are Argonne Lab, UC Santa Cruz, University of Cambridge, CIEMAT-Madrid, University of Chicago, University College London, DES-Brazil Consortium, University of Edinburgh, ETH Zurich, Fermilab, University of Illinois, ICE (IEECCSIC), IFAE Barcelona, Lawrence Berkeley Lab, LMU Munchen and the associated Excellence Cluster Universe, University of Michigan, NOAO, University of Nottingham, Ohio State University, OzDES Membership Consortium, University of Pennsylvania, University of Portsmouth, SLAC National Lab, Stanford University, University of Sussex, and Texas A&M University. Based on observations at Cerro Tololo Inter-American Observatory, National Optical Astronomy Observatory (NOAO Prop. ID 2012B-0001; PI: J. Frieman), which is operated by the Association of Universities for Research in Astronomy (AURA) under a cooperative agreement with the National

Science Foundation.

Facility: VST ESO programs: 099.D-0191, 099.D-0568, 0100.D-0022.

APPENDIX A: BRIGHT STARS SPIKES MASKING

Here we describe the procedure implemented in VST-Tube to mask haloes and spikes caused by bright stars on OmegaCam images. The spikes are due to diffraction from secondary mirror supports which in case of VST telescope are two pairs of tin supports diametrically opposite to the central secondary mirror. In case of very bright stars, too deep pixels saturation causes an overflow of charges in the pixels along the CCD reading direction. The halos are instead due to multiple reflections at optical surfaces¹². All these artifacts should be masked in order to reduce the contamination of spurious detections in the catalogues extracted from the images. The extent to which it is necessary to mask such artifacts is related to the specific analysis performed on the images. In other words the masking should be tailored as much as possible to scientific goals. Our guideline to define the masked regions are the spurious detections (with a SExtractor detection threshold of 1.5) on the difference images produced with HOTPANTS (Becker 2015). For each of the three classes of artifacts mentioned we need to adopt a specific method to create the mask. Empirically, we notice that the halo around the stars is a function of the brightness and position of the star with respect to the center of the field. In order to define this function we created a list containing stars position, magnitude and size of the haloes around the stars as determined by visual inspection. The list was used to fit a second order polynomial surface. For a given exposure time the halo size appears to be quite stable. When we need to create the mask for a new image, the first step is to obtain magnitude and position of the bright stars. For that purpose we use an external catalogue (Tycho; Høg et al. 2000), accessed through the astroquery¹³ package since the catalogue extracted with SEXtractor is not reliable for very bright stars. The radius of the halo around the bright stars obtained using function previously described, are used also to scale properly the mask of spikes. We can easily recognize that the spikes pattern is quite stable and rotates according to the camera absolute rotation angle (reported in the Fits header). The amplitude of each spike is a function of the star magnitude. We can parametrize the polygonal region that covers the spike with the camera absolute rotation angle and the halo radius (which is a function of the magnitude). Each cusp masking one spike is written as follows:

$$\begin{aligned}
 p_x &= c_x + (r + d) * \sin(\alpha) \\
 p_y &= c_y + (r + d) * \cos(\alpha) \\
 p_{px} &= c_x + r * \sin(\alpha + \beta) \\
 p_{py} &= c_y + r * \cos(\alpha + \beta) \\
 p_{mx} &= c_x + r * \sin(\alpha - \beta) \\
 p_{my} &= c_y + r * \cos(\alpha - \beta)
 \end{aligned}
 \tag{A1}$$

where c_x and c_y are the star coordinates, r is the halo radius, d is the size of the spike being considered, α is the absolute rotation angle and β is the angular width at the cusp base. In the present implementations eleven cusps are defined for each star. Fig. A1 shows an example of the mask for a bright star.

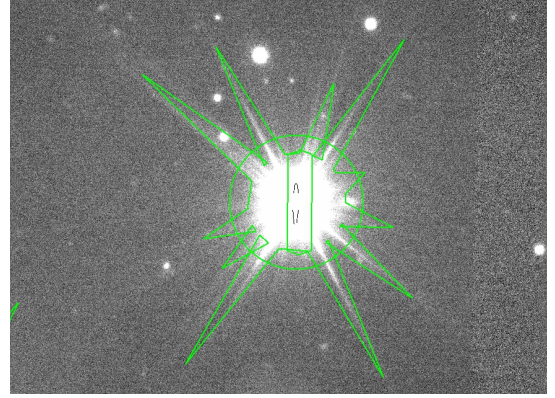


Figure A1. Example of bright star mask

APPENDIX B: TRANSIENTS

In figures B1 and B2 detailed images of the 53 transients candidates are shown. Each cut-out, extracted from the original image at the epoch of brightest magnitude, is centered on the transient and has a size of $1' \times 1'$. In table B1 is reported the transients photometry catalogue. In case of missing detection in a particular epoch, we report the limiting magnitude of the image preceded by the symbol $>$.

¹² <http://casu.ast.cam.ac.uk/surveys-projects/vista/technical/spikes-and-halos>

¹³ <https://astroquery.readthedocs.io/en/latest/>

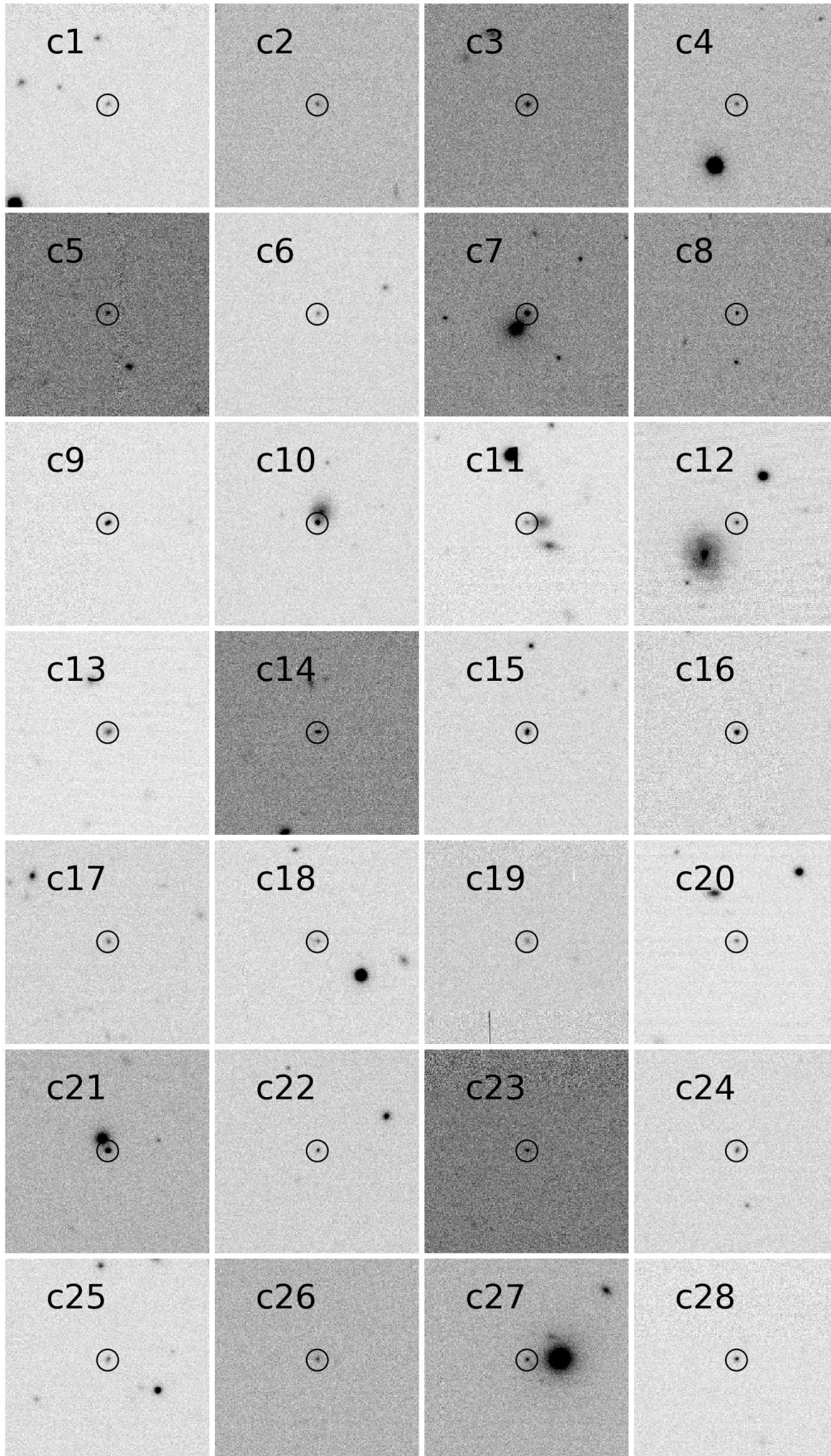


Figure B1. First 28 transient candidates found with the VST in 99 deg^2 covering the GW170814 error area. Each image has a size of $1' \times 1'$ and is extracted from the original images at the epoch of the brightest magnitude.

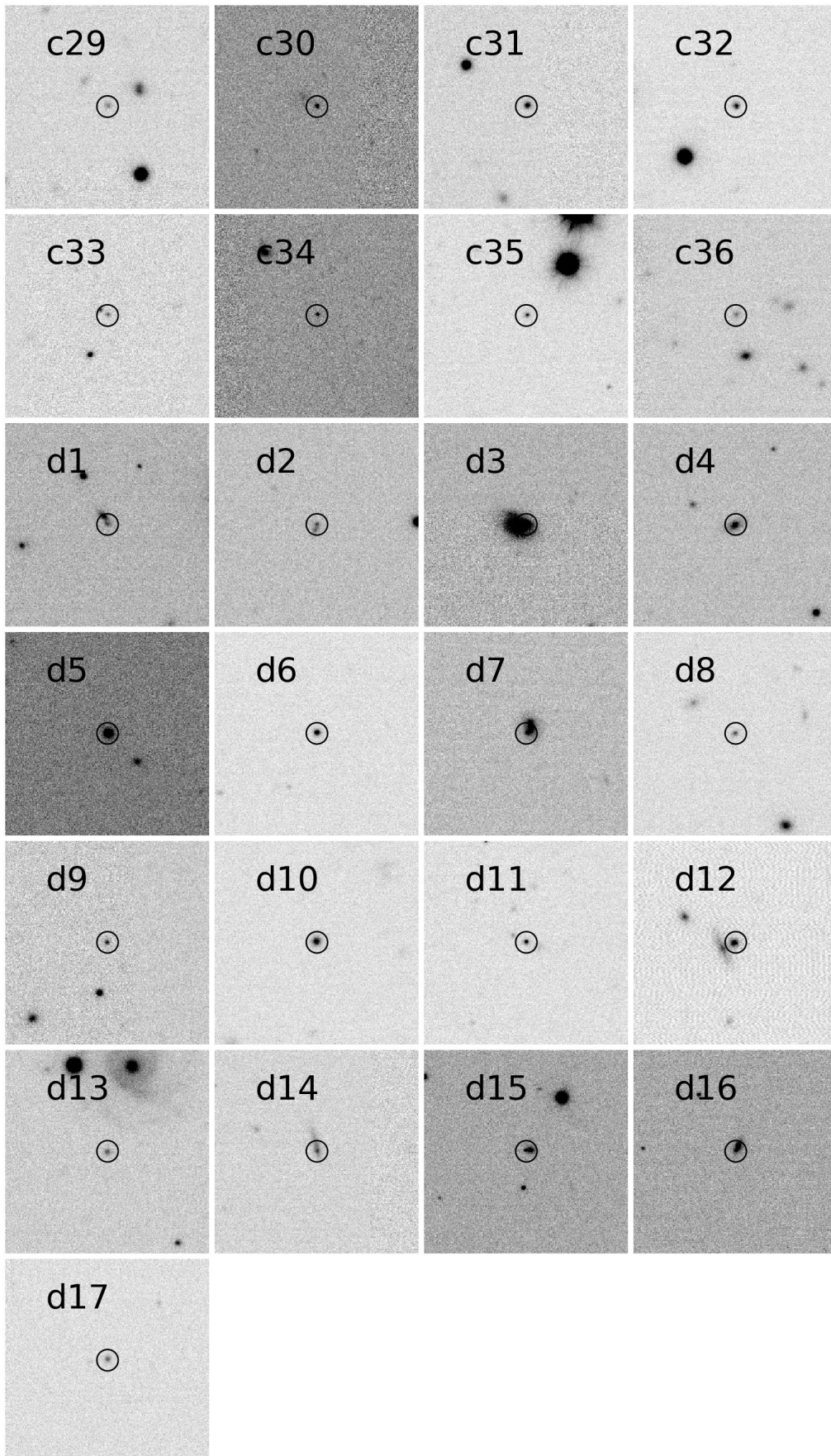


Figure B2. Images of transient candidates from c29 to d17 at the brightest magnitude. The size is $1' \times 1'$.

Table B1. Transients catalogue for the first 3 epochs. Column 1 is the identification name; columns 2 and 3 the coordinates; column 4 is the modified Julian day; column 5 the AB magnitude with the relative error. Then the modified Julian day and magnitude are repeated for the next two epochs. In the epochs without detection it is reported the limiting magnitude preceded by the symbol >.

Id	epoch 1			epoch 2		epoch 3		
	RA (deg)	DEC (deg)	MJD	MAG (AB)	MJD	MAG (AB)	MJD	MAG (AB)
c1	47.93876	-32.50572	57980.38	>21.75 ± 0.20	57982.33	>22.15 ± 0.18	57985.28	>22.13 ± 0.27
c2	41.12476	-47.08170	57980.34	20.14 ± 0.17	57982.29	20.52 ± 0.20	57985.24	20.36 ± 0.20
c3	44.24308	-36.10156	57980.35	>22.15 ± 0.23	57982.30	>22.16 ± 0.20	57985.25	>22.11 ± 0.20
c4	43.55516	-46.05383	57980.27	20.98 ± 0.19	57982.21	>21.86 ± 0.30	57984.33	>22.17 ± 0.47
c5	39.56146	-45.53453	57980.26	>22.16 ± 0.25	57982.18	>21.60 ± 0.25	57984.29	>22.25 ± 0.42
c6	44.29046	-37.11974	57980.34	19.28 ± 0.21	57982.30	20.36 ± 0.19	57985.25	19.74 ± 0.16
c7	36.37832	-46.60462	57980.20	>22.03 ± 0.25	57982.19	>21.90 ± 0.39	57984.31	>22.16 ± 0.25
c8	35.69231	-43.94526	57980.21	>22.10 ± 0.29	57982.20	>22.03 ± 0.20	57984.32	>22.16 ± 0.50
c9	40.96637	-39.09182	57980.32	>22.07 ± 0.25	57982.26	>22.13 ± 0.27	57985.36	19.15 ± 0.16
c10	42.84391	-46.75855	57980.26	19.56 ± 0.12	57982.18	19.42 ± 0.13	57984.29	19.33 ± 0.11
c11	47.22520	-33.98899	57980.37	>21.97 ± 0.29	57982.33	>22.11 ± 0.16	57985.28	>22.16 ± 0.23
c12	48.52714	-42.08370	-	---	-	---	57985.32	>21.68 ± 0.20
c13	40.71350	-38.97058	57980.32	>22.01 ± 0.22	57982.26	>22.12 ± 0.27	57985.36	>22.42 ± 0.36
c14	36.19326	-46.11161	57980.20	>22.05 ± 0.25	57982.19	>21.87 ± 0.34	57984.31	>22.09 ± 0.24
c15	49.44558	-43.49652	-	---	-	---	57985.31	>22.25 ± 0.30
c16	43.33967	-41.94081	57980.30	>22.13 ± 0.23	57982.24	>22.12 ± 0.21	57984.36	>22.05 ± 0.38
c17	42.54444	-41.49203	57980.31	>22.10 ± 0.28	57982.25	>22.10 ± 0.23	57984.37	>22.07 ± 0.34
c18	47.20362	-41.20692	-	---	-	---	57985.32	20.91 ± 0.17
c19	42.06331	-49.45406	57980.33	>22.08 ± 0.19	57982.28	>22.18 ± 0.21	57985.23	>21.75 ± 0.34
c20	36.50260	-43.98644	57980.22	20.28 ± 0.17	57982.21	20.41 ± 0.16	57984.32	20.42 ± 0.15
c21	41.17931	-40.37404	57980.31	18.89 ± 0.11	57982.25	18.45 ± 0.12	57985.35	18.96 ± 0.11
c22	36.94201	-49.98622	57980.25	>22.04 ± 0.17	57982.35	20.59 ± 0.16	57985.30	>22.10 ± 0.20
c23	42.92521	-45.71532	57980.26	>22.13 ± 0.16	57982.18	>21.52 ± 0.36	57984.29	>22.25 ± 0.32
c24	42.71470	-42.51475	57980.30	>22.01 ± 0.19	57982.24	>22.10 ± 0.25	57984.36	>22.07 ± 0.36
c25	40.17324	-46.87562	57980.29	>21.97 ± 0.32	57982.17	>21.62 ± 0.30	57984.28	>22.32 ± 0.44
c26	42.22224	-38.25838	57980.33	>21.90 ± 0.33	57982.27	>22.09 ± 0.27	57985.36	22.92 ± 0.25
c27	40.63033	-41.06565	57980.31	20.41 ± 0.12	57982.24	20.49 ± 0.13	57984.36	20.58 ± 0.16
c28	36.88136	-52.49284	57980.23	>22.16 ± 0.24	57982.34	>22.17 ± 0.22	57985.29	>22.25 ± 0.30
c29	48.50660	-42.58589	-	---	-	---	57985.32	20.29 ± 0.15
c30	35.93385	-44.02682	57980.21	>22.10 ± 0.22	57982.20	>22.02 ± 0.26	57984.32	>22.11 ± 0.23
c31	47.23585	-46.62792	57980.27	>22.05 ± 0.22	57982.22	>21.90 ± 0.35	57984.33	>22.19 ± 0.20
c32	46.59110	-38.23088	-	---	-	---	57985.34	>22.12 ± 0.29
c33	46.09634	-42.57915	-	---	-	---	57985.31	>22.20 ± 0.18
c34	38.97934	-45.03692	57980.24	>22.05 ± 0.22	57982.19	21.43 ± 0.20	57984.31	>22.14 ± 0.26
c35	38.86904	-52.55772	57980.24	>22.11 ± 0.19	57982.34	21.59 ± 0.25	57985.29	>21.99 ± 0.42
c36	39.28249	-45.36645	57980.26	>22.18 ± 0.30	57982.18	>21.58 ± 0.25	57984.29	>22.33 ± 0.41
d1	42.24100	-43.27893	57980.29	20.76 ± 0.24	57982.24	20.75 ± 0.34	57984.35	19.84 ± 0.21
d2	44.27798	-36.80744	57980.35	20.76 ± 0.20	57982.30	20.50 ± 0.17	57985.25	20.35 ± 0.15
d3	46.29475	-45.55090	57980.28	17.41 ± 0.11	57982.22	17.44 ± 0.13	57984.34	17.38 ± 0.13
d4	44.32350	-37.35107	57980.34	19.98 ± 0.17	57982.30	19.61 ± 0.15	57985.25	19.49 ± 0.14
d5	41.50049	-46.85482	57980.29	17.45 ± 0.11	57982.17	17.53 ± 0.11	57984.28	17.52 ± 0.11
d6	45.05304	-32.30412	57980.37	18.68 ± 0.11	57982.33	18.88 ± 0.11	57985.28	18.98 ± 0.11
d7	37.81450	-46.85080	57980.22	20.07 ± 0.29	57982.20	18.91 ± 0.15	57984.31	19.34 ± 0.27
d8	40.11296	-46.33456	57980.25	20.56 ± 0.17	57982.17	20.21 ± 0.15	57984.28	20.17 ± 0.14
d9	44.17079	-42.58189	57980.30	19.91 ± 0.15	57982.24	19.98 ± 0.14	57984.36	19.85 ± 0.14
d10	41.56164	-49.89749	57980.33	18.64 ± 0.12	57982.28	18.58 ± 0.12	57985.23	18.59 ± 0.12
d11	47.19114	-33.94179	57980.37	20.21 ± 0.14	57982.33	19.24 ± 0.12	57985.28	19.23 ± 0.12
d12	39.78474	-48.51388	57980.33	19.01 ± 0.15	57982.29	18.85 ± 0.13	57985.23	18.83 ± 0.12
d13	45.63721	-46.35241	57980.27	20.00 ± 0.14	57982.21	19.97 ± 0.14	57984.33	20.03 ± 0.13
d14	45.75856	-44.83118	-	---	57982.23	20.23 ± 0.17	57984.34	20.06 ± 0.17
d15	44.42912	-41.44589	57980.31	19.96 ± 0.16	57982.25	19.77 ± 0.14	57984.37	19.42 ± 0.13
d16	44.37912	-42.12675	57980.30	19.49 ± 0.18	57982.24	19.39 ± 0.17	57984.36	19.19 ± 0.14
d17	45.45381	-35.57484	57980.36	20.45 ± 0.15	57982.31	20.23 ± 0.14	57985.26	20.23 ± 0.14

Table B1. Transients catalogue for the last 3 epochs. For the description see the caption of the previous table.

Id	epoch 4				epoch 5		epoch 6	
	RA (deg)	DEC (deg)	MJD	MAG (AB)	MJD	MAG (AB)	MJD	MAG (AB)
c1	47.93876	-32.50572	57992.29	20.64 ± 0.13	58009.24	>21.64 ± 0.25	58024.36	>22.17 ± 0.28
c2	41.12476	-47.08170	57990.38	20.41 ± 0.21	58009.22	>21.71 ± 0.39	58024.17	>22.11 ± 0.21
c3	44.24308	-36.10156	57990.39	>22.20 ± 0.31	58008.38	19.82 ± 0.15	58024.19	>22.11 ± 0.16
c4	43.55516	-46.05383	57993.38	>22.54 ± 0.19	58011.19	>22.15 ± 0.25	58025.14	>22.06 ± 0.19
c5	39.56146	-45.53453	57992.34	>22.41 ± 0.34	58009.28	20.50 ± 0.16	58025.08	20.39 ± 0.16
c6	44.29046	-37.11974	57990.39	19.52 ± 0.18	58008.38	>21.51 ± 0.25	58024.18	>22.14 ± 0.19
c7	36.37832	-46.60462	57992.38	>22.07 ± 0.25	58009.30	>21.75 ± 0.32	58025.10	18.85 ± 0.12
c8	35.69231	-43.94526	57992.39	>22.15 ± 0.23	58009.31	20.30 ± 0.16	58025.11	20.47 ± 0.15
c9	40.96637	-39.09182	-	- - -	58008.36	>21.58 ± 0.23	58024.14	>21.64 ± 0.23
c10	42.84391	-46.75855	57992.34	19.23 ± 0.11	58009.28	20.03 ± 0.15	58025.08	20.63 ± 0.13
c11	47.22520	-33.98899	57992.28	21.52 ± 0.16	58009.24	19.54 ± 0.17	58024.35	19.95 ± 0.15
c12	48.52714	-42.08370	57990.33	>21.75 ± 0.33	58008.31	19.61 ± 0.16	58024.31	20.08 ± 0.14
c13	40.71350	-38.97058	-	- - -	58008.36	>21.68 ± 0.23	58024.14	>21.63 ± 0.18
c14	36.19326	-46.11161	57992.38	>22.06 ± 0.20	58009.30	>21.75 ± 0.30	58025.10	20.11 ± 0.15
c15	49.44558	-43.49652	57990.33	>21.75 ± 0.37	58008.31	>21.25 ± 0.27	58024.31	19.41 ± 0.14
c16	43.33967	-41.94081	57990.36	>22.48 ± 0.35	58011.23	19.25 ± 0.12	58025.17	>22.14 ± 0.15
c17	42.54444	-41.49203	57990.36	>22.27 ± 0.49	58011.23	20.34 ± 0.14	58025.17	>22.09 ± 0.32
c18	47.20362	-41.20692	57990.34	>21.98 ± 0.31	58008.32	>21.60 ± 0.26	58024.32	>22.09 ± 0.19
c19	42.06331	-49.45406	57990.37	>22.15 ± 0.31	58009.20	20.14 ± 0.14	58024.16	>21.98 ± 0.28
c20	36.50260	-43.98644	57992.39	20.88 ± 0.16	58009.32	21.76 ± 0.33	58025.11	22.33 ± 0.33
c21	41.17931	-40.37404	-	- - -	58008.36	19.40 ± 0.13	58024.14	19.58 ± 0.12
c22	36.94201	-49.98622	57992.37	>22.06 ± 0.24	58009.27	>21.75 ± 0.25	58024.38	>22.19 ± 0.21
c23	42.92521	-45.71532	57992.34	>21.75 ± 0.29	58009.29	21.27 ± 0.21	58025.09	>21.90 ± 0.34
c24	42.71470	-42.51475	57990.35	>22.02 ± 0.25	58011.22	20.16 ± 0.14	58025.17	>22.09 ± 0.25
c25	40.17324	-46.87562	57992.33	20.27 ± 0.15	58009.28	>21.75 ± 0.36	58025.08	>21.70 ± 0.25
c26	42.22224	-38.25838	-	- - -	58008.37	20.09 ± 0.19	58024.15	20.57 ± 0.16
c27	40.63033	-41.06565	57990.36	21.43 ± 0.14	58011.23	21.34 ± 0.20	58025.17	21.78 ± 0.14
c28	36.88136	-52.49284	57992.36	>22.25 ± 0.34	58009.25	20.59 ± 0.14	58024.37	19.90 ± 0.11
c29	48.50660	-42.58589	57990.33	>21.75 ± 0.42	58008.31	>21.41 ± 0.34	58024.31	>22.25 ± 0.26
c30	35.93385	-44.02682	57992.39	20.34 ± 0.16	58009.31	18.70 ± 0.13	58025.11	19.50 ± 0.13
c31	47.23585	-46.62792	57993.38	>22.59 ± 0.21	58011.19	18.79 ± 0.12	58025.14	19.60 ± 0.11
c32	46.59110	-38.23088	57990.31	21.50 ± 0.23	58008.34	18.54 ± 0.12	58024.33	19.26 ± 0.12
c33	46.09634	-42.57915	57990.33	>21.82 ± 0.34	58008.31	>21.25 ± 0.30	58024.31	20.42 ± 0.16
c34	38.97934	-45.03692	57992.36	>22.06 ± 0.25	58009.29	>21.81 ± 0.36	58025.10	20.19 ± 0.14
c35	38.86904	-52.55772	57992.36	>22.08 ± 0.21	58009.26	20.43 ± 0.16	58024.37	17.94 ± 0.13
c36	39.28249	-45.36645	57992.34	>22.25 ± 0.30	58009.28	20.05 ± 0.15	58025.08	>21.75 ± 0.25
d1	42.24100	-43.27893	57990.35	19.97 ± 0.24	58011.21	20.58 ± 0.35	58025.16	22.66 ± 0.49
d2	44.27798	-36.80744	57990.39	20.46 ± 0.16	58008.38	20.20 ± 0.20	58024.19	20.45 ± 0.21
d3	46.29475	-45.55090	57993.39	17.78 ± 0.12	58011.20	17.97 ± 0.12	58025.15	18.28 ± 0.12
d4	44.32350	-37.35107	57990.39	19.64 ± 0.15	58008.38	19.27 ± 0.14	58024.18	19.46 ± 0.17
d5	41.50049	-46.85482	57992.33	17.52 ± 0.11	58009.28	17.43 ± 0.11	58025.08	17.17 ± 0.11
d6	45.05304	-32.30412	57992.28	19.00 ± 0.11	58009.24	19.00 ± 0.12	58024.35	18.24 ± 0.11
d7	37.81450	-46.85080	57992.38	19.16 ± 0.22	58009.31	18.81 ± 0.15	58025.10	21.11 ± 0.28
d8	40.11296	-46.33456	57992.33	20.15 ± 0.15	58009.28	20.84 ± 0.19	58025.08	21.21 ± 0.22
d9	44.17079	-42.58189	57990.36	20.16 ± 0.15	58011.23	20.62 ± 0.15	58025.17	21.05 ± 0.22
d10	41.56164	-49.89749	57990.37	18.61 ± 0.12	58009.20	19.21 ± 0.12	58024.16	19.35 ± 0.13
d11	47.19114	-33.94179	57992.28	19.71 ± 0.12	58009.24	19.21 ± 0.12	58024.35	19.49 ± 0.12
d12	39.78474	-48.51388	57990.38	18.80 ± 0.13	58009.21	19.02 ± 0.12	58024.17	19.25 ± 0.14
d13	45.63721	-46.35241	57993.38	20.13 ± 0.14	58011.19	20.44 ± 0.14	58025.14	20.88 ± 0.20
d14	45.75856	-44.83118	57993.40	20.99 ± 0.23	58011.20	20.09 ± 0.17	58025.15	19.75 ± 0.15
d15	44.42912	-41.44589	57990.36	19.85 ± 0.16	58011.23	19.85 ± 0.15	58025.17	20.74 ± 0.23
d16	44.37912	-42.12675	57990.36	19.26 ± 0.15	58011.23	19.49 ± 0.18	58025.17	20.77 ± 0.32
d17	45.45381	-35.57484	57990.40	20.18 ± 0.14	58008.39	20.29 ± 0.19	58024.20	20.77 ± 0.16

APPENDIX C: DETAILS ON THE POINTINGS

In the Table C1 we report details on the observations for each pointing i.e. input images names, as reported in the ESO archive, coordinates center, modified Julian day at the start time of the first image, percentage of the masked area due to bright stars, bad columns and gaps among ccds not covered by the dithering, skymap enclosed probability and 50% completeness for point-like sources.

Table C1: Details on observations for each pointing.

Image 1	Image 2	Ra	Dec	MJD	Masked	Encl.	Compl.
		(deg)	(deg)		(%)	prob. (%)	(AB)
OMEGA.2017-08-15T05:07:05.219	OMEGA.2017-08-15T05:08:30.230	35.4016	-44.3820	57980.2133	7.73	0.00004	22.16
OMEGA.2017-08-15T04:58:38.518	OMEGA.2017-08-15T05:00:03.138	35.3759	-45.4200	57980.2074	3.29	0.00007	22.07
OMEGA.2017-08-15T04:50:12.206	OMEGA.2017-08-15T04:51:36.286	35.3496	-46.4579	57980.2015	3.04	0.00005	22.02
OMEGA.2017-08-15T05:41:45.265	OMEGA.2017-08-15T05:43:09.485	35.7322	-51.4176	57980.2373	5.75	0.00010	22.04
OMEGA.2017-08-15T05:33:18.024	OMEGA.2017-08-15T05:34:42.174	35.6953	-52.4555	57980.2315	4.66	0.00009	22.20
OMEGA.2017-08-15T05:50:11.886	OMEGA.2017-08-15T05:51:36.127	35.7677	-50.3796	57980.2432	6.27	0.00014	22.04
OMEGA.2017-08-15T05:09:54.680	OMEGA.2017-08-15T05:11:18.930	36.8291	-44.3905	57980.2152	2.99	0.00025	22.02
OMEGA.2017-08-15T05:01:27.498	OMEGA.2017-08-15T05:02:51.668	36.8292	-45.4287	57980.2093	7.43	0.00038	22.09
OMEGA.2017-08-15T04:53:00.626	OMEGA.2017-08-15T04:54:24.907	36.8300	-46.4669	57980.2035	4.67	0.00055	21.99
OMEGA.2017-08-15T05:53:00.627	OMEGA.2017-08-15T05:54:24.998	37.3676	-50.3902	57980.2451	6.36	0.00131	21.95
OMEGA.2017-08-15T05:44:34.335	OMEGA.2017-08-15T05:45:58.556	37.3680	-51.4284	57980.2393	5.54	0.00116	21.99
OMEGA.2017-08-15T05:36:06.945	OMEGA.2017-08-15T05:37:31.195	37.3692	-52.4666	57980.2334	4.26	0.00085	22.05
OMEGA.2017-08-15T05:27:36.813	OMEGA.2017-08-15T05:29:05.243	38.2181	-48.4189	57980.2275	4.10	0.00272	22.11
OMEGA.2017-08-15T05:15:32.631	OMEGA.2017-08-15T05:16:56.691	38.1871	-49.4568	57980.2191	3.84	0.00345	22.15
OMEGA.2017-08-15T05:12:43.570	OMEGA.2017-08-15T05:14:07.790	38.2565	-44.3809	57980.2172	8.92	0.00080	22.11
OMEGA.2017-08-15T05:30:29.453	OMEGA.2017-08-15T05:31:53.664	38.2482	-47.3808	57980.2295	8.80	0.00210	22.11
OMEGA.2017-08-15T05:04:16.698	OMEGA.2017-08-15T05:05:40.938	38.2824	-45.4189	57980.2113	6.63	0.00135	22.09
OMEGA.2017-08-15T04:55:50.037	OMEGA.2017-08-15T04:57:14.117	38.3106	-46.4570	57980.2054	3.18	0.00216	22.11
OMEGA.2017-08-15T05:55:49.697	OMEGA.2017-08-15T05:57:13.928	38.9676	-50.3784	57980.2471	10.68	0.00419	21.98
OMEGA.2017-08-15T05:47:23.086	OMEGA.2017-08-15T05:48:47.666	39.0038	-51.4163	57980.2412	3.15	0.00350	22.01
OMEGA.2017-08-15T05:38:55.475	OMEGA.2017-08-15T05:40:19.995	39.0430	-52.4542	57980.2354	5.30	0.00206	22.09
OMEGA.2017-08-15T05:58:38.318	OMEGA.2017-08-15T06:00:02.538	39.6292	-46.4580	57980.2491	3.47	0.00340	22.03
OMEGA.2017-08-15T06:20:29.502	OMEGA.2017-08-15T06:21:55.502	39.6813	-44.3820	57980.2642	10.72	0.00151	22.10
OMEGA.2017-08-15T06:12:02.410	OMEGA.2017-08-15T06:13:26.881	39.6556	-45.4200	57980.2584	4.71	0.00224	22.21
OMEGA.2017-08-15T08:07:36.281	OMEGA.2017-08-15T08:09:00.592	39.7549	-47.3903	57980.3386	5.09	0.00478	22.27
OMEGA.2017-08-15T07:57:55.519	OMEGA.2017-08-15T07:59:19.669	39.7551	-48.4285	57980.3319	4.92	0.00593	22.06
OMEGA.2017-08-15T05:24:31.012	OMEGA.2017-08-15T05:25:55.062	39.7562	-49.4667	57980.2254	4.17	0.00645	22.01
OMEGA.2017-08-15T07:38:06.916	OMEGA.2017-08-15T07:39:32.012	41.1409	-39.4220	57980.3181	4.70	0.00005	21.99
OMEGA.2017-08-15T07:29:40.074	OMEGA.2017-08-15T07:31:04.505	41.1216	-40.4600	57980.3123	3.26	0.00012	22.04
OMEGA.2017-08-15T07:21:14.763	OMEGA.2017-08-15T07:22:38.823	41.1031	-41.3874	57980.3064	8.01	0.00022	22.11
OMEGA.2017-08-15T07:02:41.590	OMEGA.2017-08-15T07:04:06.390	41.0812	-42.4233	57980.2935	5.85	0.00039	21.96
OMEGA.2017-08-15T06:54:15.658	OMEGA.2017-08-15T06:55:39.738	41.0587	-43.4590	57980.2877	2.96	0.00075	22.00
OMEGA.2017-08-15T06:23:19.502	OMEGA.2017-08-15T06:24:43.503	41.1088	-44.3905	57980.2662	6.47	0.00146	22.13
OMEGA.2017-08-15T06:14:50.951	OMEGA.2017-08-15T06:16:17.531	41.1089	-45.4287	57980.2603	3.70	0.00236	22.07
OMEGA.2017-08-15T06:06:18.770	OMEGA.2017-08-15T06:07:43.080	41.1098	-46.4669	57980.2544	3.97	0.00346	21.94
OMEGA.2017-08-15T07:46:34.437	OMEGA.2017-08-15T07:47:59.307	41.1599	-38.3839	57980.3240	7.63	0.00001	21.94
OMEGA.2017-08-15T08:10:25.251	OMEGA.2017-08-15T08:11:49.952	41.2616	-47.3798	57980.3406	6.74	0.00456	22.20
OMEGA.2017-08-15T08:04:47.950	OMEGA.2017-08-15T08:06:12.061	41.2923	-48.4177	57980.3367	4.94	0.00526	22.06
OMEGA.2017-08-15T07:55:06.978	OMEGA.2017-08-15T07:56:31.279	41.3252	-49.4557	57980.3299	3.43	0.00534	21.99
OMEGA.2017-08-15T07:49:23.388	OMEGA.2017-08-15T07:50:47.638	42.4613	-38.3907	57980.3260	9.02	0.00000	21.86
OMEGA.2017-08-15T07:40:56.626	OMEGA.2017-08-15T07:42:20.886	42.4613	-39.4290	57980.3201	7.66	0.00001	22.04
OMEGA.2017-08-15T07:32:28.495	OMEGA.2017-08-15T07:33:53.365	42.4619	-40.4672	57980.3142	2.98	0.00002	21.98
OMEGA.2017-08-15T07:24:02.913	OMEGA.2017-08-15T07:25:27.253	42.4621	-41.3951	57980.3084	6.29	0.00005	22.17
OMEGA.2017-08-15T07:15:37.512	OMEGA.2017-08-15T07:17:01.842	42.4620	-42.4311	57980.3025	5.06	0.00016	22.04
OMEGA.2017-08-15T06:57:03.788	OMEGA.2017-08-15T06:58:28.168	42.4628	-43.4671	57980.2896	5.30	0.00043	21.94
OMEGA.2017-08-15T06:26:07.513	OMEGA.2017-08-15T06:27:31.523	42.5363	-44.3809	57980.2681	9.31	0.00092	22.07
OMEGA.2017-08-15T06:17:41.542	OMEGA.2017-08-15T06:19:05.512	42.5621	-45.4189	57980.2623	4.75	0.00143	22.11
OMEGA.2017-08-15T06:09:13.950	OMEGA.2017-08-15T06:10:38.181	42.5903	-46.4570	57980.2564	4.13	0.00220	21.99
OMEGA.2017-08-15T08:21:44.133	OMEGA.2017-08-15T08:23:08.614	43.7420	-36.4228	57980.3484	5.17	0.00000	22.08
OMEGA.2017-08-15T08:13:18.062	OMEGA.2017-08-15T08:14:42.272	43.7254	-37.4609	57980.3426	2.94	0.00000	22.18
OMEGA.2017-08-15T08:30:10.845	OMEGA.2017-08-15T08:31:35.495	43.7584	-35.3847	57980.3543	5.36	0.00000	22.11
OMEGA.2017-08-15T07:52:11.928	OMEGA.2017-08-15T07:53:36.169	43.7627	-38.3830	57980.3279	5.50	0.00000	22.07

OMEGA.2017-08-15T07:43:46.017	OMEGA.2017-08-15T07:45:10.217	43.7817	-39.4211	57980.3221	6.07	0.00004	22.18
OMEGA.2017-08-15T07:35:18.295	OMEGA.2017-08-15T07:36:42.526	43.8023	-40.4591	57980.3162	4.05	0.00006	21.94
OMEGA.2017-08-15T07:26:51.394	OMEGA.2017-08-15T07:28:15.504	43.8209	-41.3865	57980.3103	4.78	0.00006	22.10
OMEGA.2017-08-15T07:18:26.512	OMEGA.2017-08-15T07:19:50.682	43.8430	-42.4224	57980.3045	4.03	0.00022	21.98
OMEGA.2017-08-15T06:59:53.119	OMEGA.2017-08-15T07:01:17.509	43.8670	-43.4581	57980.2916	5.67	0.00080	22.03
OMEGA.2017-08-15T06:37:21.265	OMEGA.2017-08-15T06:38:45.675	43.9353	-45.4222	57980.2759	4.69	0.00235	22.01
OMEGA.2017-08-15T06:28:55.863	OMEGA.2017-08-15T06:30:20.094	43.9091	-46.4579	57980.2701	3.38	0.00504	22.05
OMEGA.2017-08-15T06:45:46.867	OMEGA.2017-08-15T06:47:11.087	43.9609	-44.3864	57980.2818	5.28	0.00116	22.09
OMEGA.2017-08-15T08:55:31.540	OMEGA.2017-08-15T08:56:55.780	44.9953	-32.7019	57980.3719	9.38	0.00000	22.16
OMEGA.2017-08-15T08:47:05.678	OMEGA.2017-08-15T08:48:29.898	44.9809	-33.7401	57980.3660	6.76	0.00000	21.93
OMEGA.2017-08-15T08:38:38.717	OMEGA.2017-08-15T08:40:03.206	44.9664	-34.7783	57980.3602	3.79	0.00000	22.03
OMEGA.2017-08-15T08:32:59.666	OMEGA.2017-08-15T08:34:24.146	45.0096	-35.3909	57980.3562	4.50	0.00000	22.12
OMEGA.2017-08-15T08:24:32.834	OMEGA.2017-08-15T08:25:57.054	45.0095	-36.4291	57980.3504	6.44	0.00000	22.22
OMEGA.2017-08-15T08:16:06.502	OMEGA.2017-08-15T08:17:30.673	45.0101	-37.4673	57980.3445	6.28	0.00002	22.05
OMEGA.2017-08-15T06:48:35.317	OMEGA.2017-08-15T06:49:59.667	45.3876	-44.3950	57980.2837	5.40	0.00848	22.02
OMEGA.2017-08-15T06:40:09.826	OMEGA.2017-08-15T06:41:34.306	45.3877	-45.4309	57980.2779	3.13	0.01770	22.05
OMEGA.2017-08-15T06:31:44.524	OMEGA.2017-08-15T06:33:08.734	45.3885	-46.4669	57980.2720	2.87	0.02424	22.01
OMEGA.2017-08-15T08:58:20.319	OMEGA.2017-08-15T08:59:44.690	46.2075	-32.7077	57980.3738	10.23	0.00000	21.84
OMEGA.2017-08-15T08:49:54.129	OMEGA.2017-08-15T08:51:18.358	46.2075	-33.7459	57980.3680	4.44	0.00000	21.78
OMEGA.2017-08-15T08:41:27.447	OMEGA.2017-08-15T08:42:51.697	46.2080	-34.7841	57980.3621	4.47	0.00001	21.85
OMEGA.2017-08-15T08:35:50.226	OMEGA.2017-08-15T08:37:14.436	46.3160	-35.2259	57980.3582	2.83	0.00002	22.15
OMEGA.2017-08-15T08:27:22.194	OMEGA.2017-08-15T08:28:46.624	46.2771	-36.4220	57980.3523	4.22	0.00006	22.01
OMEGA.2017-08-15T08:18:55.423	OMEGA.2017-08-15T08:20:19.913	46.2949	-37.4602	57980.3465	4.26	0.00020	22.14
OMEGA.2017-08-15T06:51:23.907	OMEGA.2017-08-15T06:52:48.278	46.8143	-44.3854	57980.2857	11.74	0.03689	22.01
OMEGA.2017-08-15T06:42:58.526	OMEGA.2017-08-15T06:44:22.816	46.8401	-45.4212	57980.2798	6.72	0.05186	21.96
OMEGA.2017-08-15T06:34:32.804	OMEGA.2017-08-15T06:35:57.024	46.8681	-46.4569	57980.2740	5.42	0.05280	22.04
OMEGA.2017-08-15T09:01:08.901	OMEGA.2017-08-15T09:02:33.121	47.4198	-32.7013	57980.3758	6.45	0.00000	21.93
OMEGA.2017-08-15T08:52:42.829	OMEGA.2017-08-15T08:54:07.059	47.4340	-33.7395	57980.3699	7.14	0.00001	21.80
OMEGA.2017-08-15T08:44:15.918	OMEGA.2017-08-15T08:45:40.168	47.4495	-34.7776	57980.3641	5.07	0.00013	21.89
OMEGA.2017-08-17T04:52:35.160	OMEGA.2017-08-17T04:53:59.430	35.4016	-44.3820	57982.2032	3.52	0.00007	21.98
OMEGA.2017-08-17T04:44:08.889	OMEGA.2017-08-17T04:45:33.179	35.3759	-45.4200	57982.1973	3.07	0.00009	21.93
OMEGA.2017-08-17T04:35:40.297	OMEGA.2017-08-17T04:37:04.488	35.3496	-46.4579	57982.1914	3.03	0.00005	21.95
OMEGA.2017-08-17T08:11:42.045	OMEGA.2017-08-17T08:13:06.275	35.7322	-51.4176	57982.3415	3.39	0.00013	22.25
OMEGA.2017-08-17T08:03:16.353	OMEGA.2017-08-17T08:04:40.713	35.6953	-52.4555	57982.3356	3.33	0.00010	22.30
OMEGA.2017-08-17T08:20:07.856	OMEGA.2017-08-17T08:21:32.097	35.7677	-50.3796	57982.3473	3.85	0.00021	22.21
OMEGA.2017-08-17T04:55:23.680	OMEGA.2017-08-17T04:56:47.981	36.8291	-44.3905	57982.2051	2.89	0.00031	22.03
OMEGA.2017-08-17T04:46:57.509	OMEGA.2017-08-17T04:48:21.760	36.8292	-45.4287	57982.1993	4.87	0.00042	21.67
OMEGA.2017-08-17T04:38:28.738	OMEGA.2017-08-17T04:39:53.009	36.8300	-46.4669	57982.1934	3.00	0.00054	21.96
OMEGA.2017-08-17T08:22:56.847	OMEGA.2017-08-17T08:24:21.087	37.3676	-50.3902	57982.3493	4.01	0.00175	22.21
OMEGA.2017-08-17T08:14:30.856	OMEGA.2017-08-17T08:15:55.096	37.3680	-51.4284	57982.3434	4.09	0.00135	22.21
OMEGA.2017-08-17T08:06:04.984	OMEGA.2017-08-17T08:07:29.504	37.3692	-52.4666	57982.3376	4.42	0.00086	22.20
OMEGA.2017-08-17T06:48:03.410	OMEGA.2017-08-17T06:49:27.500	38.2181	-48.4189	57982.2834	3.55	0.00301	22.25
OMEGA.2017-08-17T06:39:37.379	OMEGA.2017-08-17T06:41:01.639	38.1871	-49.4568	57982.2775	4.83	0.00353	22.06
OMEGA.2017-08-17T04:58:12.052	OMEGA.2017-08-17T04:59:36.301	38.2565	-44.3809	57982.2071	2.82	0.00088	21.87
OMEGA.2017-08-17T06:56:28.911	OMEGA.2017-08-17T06:57:53.612	38.2482	-47.3808	57982.2892	3.63	0.00257	22.24
OMEGA.2017-08-17T04:49:46.011	OMEGA.2017-08-17T04:51:10.410	38.2824	-45.4189	57982.2012	3.75	0.00140	21.72
OMEGA.2017-08-17T04:41:19.358	OMEGA.2017-08-17T04:42:43.608	38.3106	-46.4570	57982.1954	3.37	0.00207	21.56
OMEGA.2017-08-17T08:25:45.468	OMEGA.2017-08-17T08:27:09.758	38.9676	-50.3784	57982.3512	2.94	0.00462	22.40
OMEGA.2017-08-17T08:17:19.326	OMEGA.2017-08-17T08:18:43.627	39.0038	-51.4163	57982.3454	3.10	0.00368	22.35
OMEGA.2017-08-17T08:08:53.755	OMEGA.2017-08-17T08:10:17.955	39.0430	-52.4542	57982.3395	4.70	0.00213	22.03
OMEGA.2017-08-17T04:06:59.212	OMEGA.2017-08-17T04:08:23.472	39.6292	-46.4580	57982.1715	3.48	0.00345	21.70
OMEGA.2017-08-17T04:23:53.305	OMEGA.2017-08-17T04:25:17.535	39.6813	-44.3820	57982.1833	5.50	0.00161	21.63
OMEGA.2017-08-17T04:15:27.514	OMEGA.2017-08-17T04:16:51.844	39.6556	-45.4200	57982.1774	4.56	0.00234	21.64
OMEGA.2017-08-17T06:59:18.043	OMEGA.2017-08-17T07:00:42.642	39.7549	-47.3903	57982.2912	3.52	0.00497	22.30
OMEGA.2017-08-17T06:50:52.090	OMEGA.2017-08-17T06:52:16.291	39.7551	-48.4285	57982.2853	3.13	0.00594	22.05
OMEGA.2017-08-17T06:42:25.939	OMEGA.2017-08-17T06:43:50.200	39.7562	-49.4667	57982.2795	4.27	0.00612	22.12
OMEGA.2017-08-17T06:14:34.494	OMEGA.2017-08-17T06:15:59.006	41.1409	-39.4220	57982.2601	2.98	0.00005	22.12
OMEGA.2017-08-17T06:06:08.873	OMEGA.2017-08-17T06:07:33.094	41.1216	-40.4600	57982.2543	3.14	0.00012	22.05
OMEGA.2017-08-17T05:52:32.230	OMEGA.2017-08-17T05:53:56.491	41.1031	-41.3874	57982.2448	3.42	0.00017	22.23
OMEGA.2017-08-17T05:44:05.869	OMEGA.2017-08-17T05:45:30.249	41.0812	-42.4233	57982.2390	3.39	0.00036	22.19
OMEGA.2017-08-17T05:35:38.528	OMEGA.2017-08-17T05:37:02.798	41.0587	-43.4590	57982.2331	3.27	0.00076	22.06
OMEGA.2017-08-17T04:26:42.056	OMEGA.2017-08-17T04:28:06.296	41.1088	-44.3905	57982.1852	3.59	0.00128	21.75

OMEGA.2017-08-17T04:18:16.094	OMEGA.2017-08-17T04:19:40.615	41.1089	-45.4287	57982.1794	3.17	0.00224	21.58
OMEGA.2017-08-17T04:09:48.253	OMEGA.2017-08-17T04:11:14.493	41.1098	-46.4669	57982.1735	4.30	0.00327	21.65
OMEGA.2017-08-17T06:23:00.336	OMEGA.2017-08-17T06:24:24.506	41.1599	-38.3839	57982.2660	3.91	0.00001	22.19
OMEGA.2017-08-17T07:02:06.862	OMEGA.2017-08-17T07:03:31.043	41.2616	-47.3798	57982.2931	3.59	0.00410	21.97
OMEGA.2017-08-17T06:53:40.481	OMEGA.2017-08-17T06:55:04.741	41.2923	-48.4177	57982.2873	3.56	0.00496	22.05
OMEGA.2017-08-17T06:45:14.690	OMEGA.2017-08-17T06:46:38.950	41.3252	-49.4557	57982.2814	3.82	0.00527	22.19
OMEGA.2017-08-17T06:25:48.887	OMEGA.2017-08-17T06:27:14.377	42.4613	-38.3907	57982.2679	3.54	0.00000	22.09
OMEGA.2017-08-17T06:17:23.495	OMEGA.2017-08-17T06:18:47.925	42.4613	-39.4290	57982.2621	3.14	0.00001	22.22
OMEGA.2017-08-17T06:08:57.413	OMEGA.2017-08-17T06:10:21.664	42.4619	-40.4672	57982.2562	2.97	0.00002	22.22
OMEGA.2017-08-17T05:55:21.011	OMEGA.2017-08-17T05:56:45.952	42.4621	-41.3951	57982.2468	4.33	0.00004	22.19
OMEGA.2017-08-17T05:46:54.500	OMEGA.2017-08-17T05:48:19.240	42.4620	-42.4311	57982.2409	4.46	0.00015	22.16
OMEGA.2017-08-17T05:38:27.398	OMEGA.2017-08-17T05:39:51.788	42.4628	-43.4671	57982.2350	3.25	0.00041	22.07
OMEGA.2017-08-17T04:29:30.376	OMEGA.2017-08-17T04:30:55.286	42.5363	-44.3809	57982.1872	3.65	0.00083	21.58
OMEGA.2017-08-17T04:21:04.864	OMEGA.2017-08-17T04:22:29.055	42.5621	-45.4189	57982.1813	3.49	0.00136	21.40
OMEGA.2017-08-17T04:12:38.743	OMEGA.2017-08-17T04:14:03.014	42.5903	-46.4570	57982.1754	3.98	0.00211	21.50
OMEGA.2017-08-17T07:16:35.486	OMEGA.2017-08-17T07:18:00.176	43.7420	-36.4228	57982.3032	3.88	0.00000	22.16
OMEGA.2017-08-17T07:08:07.984	OMEGA.2017-08-17T07:09:32.274	43.7254	-37.4609	57982.2973	2.99	0.00000	22.05
OMEGA.2017-08-17T07:25:01.347	OMEGA.2017-08-17T07:26:26.227	43.7584	-35.3847	57982.3090	3.49	0.00000	22.02
OMEGA.2017-08-17T06:28:38.657	OMEGA.2017-08-17T06:30:03.057	43.7627	-38.3830	57982.2699	3.70	0.00000	22.01
OMEGA.2017-08-17T06:20:12.145	OMEGA.2017-08-17T06:21:36.216	43.7817	-39.4211	57982.2640	3.32	0.00004	22.06
OMEGA.2017-08-17T06:11:46.214	OMEGA.2017-08-17T06:13:10.334	43.8023	-40.4591	57982.2582	4.13	0.00006	21.99
OMEGA.2017-08-17T05:58:10.172	OMEGA.2017-08-17T05:59:34.672	43.8209	-41.3865	57982.2487	3.20	0.00007	22.15
OMEGA.2017-08-17T05:49:43.470	OMEGA.2017-08-17T05:51:07.701	43.8430	-42.4224	57982.2429	4.59	0.00023	22.07
OMEGA.2017-08-17T05:41:16.518	OMEGA.2017-08-17T05:42:40.799	43.8670	-43.4581	57982.2370	2.92	0.00077	22.04
OMEGA.2017-08-17T05:14:48.554	OMEGA.2017-08-17T05:16:13.075	43.9353	-45.4222	57982.2186	3.55	0.00287	21.94
OMEGA.2017-08-17T05:06:21.452	OMEGA.2017-08-17T05:07:45.553	43.9091	-46.4579	57982.2127	3.74	0.00520	22.00
OMEGA.2017-08-17T05:23:15.165	OMEGA.2017-08-17T05:24:39.426	43.9609	-44.3864	57982.2245	3.67	0.00152	21.95
OMEGA.2017-08-17T07:52:03.171	OMEGA.2017-08-17T07:53:27.832	44.9953	-32.7019	57982.3278	4.11	0.00000	22.16
OMEGA.2017-08-17T07:43:37.420	OMEGA.2017-08-17T07:45:01.680	44.9809	-33.7401	57982.3220	3.68	0.00000	22.01
OMEGA.2017-08-17T07:35:11.368	OMEGA.2017-08-17T07:36:35.599	44.9664	-34.7783	57982.3161	3.36	0.00000	22.01
OMEGA.2017-08-17T07:27:50.448	OMEGA.2017-08-17T07:29:14.707	45.0096	-35.3909	57982.3110	4.14	0.00000	22.16
OMEGA.2017-08-17T07:19:24.466	OMEGA.2017-08-17T07:20:48.727	45.0095	-36.4291	57982.3051	3.10	0.00000	22.21
OMEGA.2017-08-17T07:10:56.474	OMEGA.2017-08-17T07:12:22.415	45.0101	-37.4673	57982.2993	3.86	0.00002	22.07
OMEGA.2017-08-17T05:26:03.686	OMEGA.2017-08-17T05:27:28.516	45.3876	-44.3950	57982.2264	3.46	0.01140	21.78
OMEGA.2017-08-17T05:17:37.315	OMEGA.2017-08-17T05:19:02.165	45.3877	-45.4309	57982.2206	3.06	0.01962	21.92
OMEGA.2017-08-17T05:09:10.073	OMEGA.2017-08-17T05:10:34.343	45.3885	-46.4669	57982.2147	2.83	0.02400	21.90
OMEGA.2017-08-17T07:54:52.092	OMEGA.2017-08-17T07:56:16.162	46.2075	-32.7077	57982.3298	4.01	0.00000	22.23
OMEGA.2017-08-17T07:46:25.840	OMEGA.2017-08-17T07:47:50.071	46.2075	-33.7459	57982.3239	3.34	0.00000	22.39
OMEGA.2017-08-17T07:37:59.839	OMEGA.2017-08-17T07:39:24.229	46.2080	-34.7841	57982.3181	3.46	0.00001	22.20
OMEGA.2017-08-17T07:30:38.877	OMEGA.2017-08-17T07:32:03.118	46.3160	-35.2259	57982.3129	2.85	0.00003	22.14
OMEGA.2017-08-17T07:22:13.076	OMEGA.2017-08-17T07:23:37.307	46.2771	-36.4220	57982.3071	3.89	0.00007	22.09
OMEGA.2017-08-17T07:13:46.725	OMEGA.2017-08-17T07:15:10.965	46.2949	-37.4602	57982.3012	4.32	0.00019	22.05
OMEGA.2017-08-17T05:28:52.777	OMEGA.2017-08-17T05:30:17.037	46.8143	-44.3854	57982.2284	3.20	0.04152	21.63
OMEGA.2017-08-17T05:20:26.425	OMEGA.2017-08-17T05:21:50.556	46.8401	-45.4212	57982.2225	3.55	0.05427	21.80
OMEGA.2017-08-17T05:11:59.654	OMEGA.2017-08-17T05:13:24.074	46.8681	-46.4569	57982.2167	4.33	0.05252	21.82
OMEGA.2017-08-17T07:57:40.842	OMEGA.2017-08-17T07:59:05.232	47.4198	-32.7013	57982.3317	2.97	0.00000	22.18
OMEGA.2017-08-17T07:49:14.161	OMEGA.2017-08-17T07:50:38.681	47.4340	-33.7395	57982.3259	2.96	0.00001	22.11
OMEGA.2017-08-17T07:40:48.880	OMEGA.2017-08-17T07:42:13.190	47.4495	-34.7776	57982.3200	3.47	0.00012	22.10
OMEGA.2017-08-19T07:36:36.020	OMEGA.2017-08-19T07:38:01.259	35.4016	-44.3820	57984.3171	3.17	0.00007	21.67
OMEGA.2017-08-19T07:28:10.318	OMEGA.2017-08-19T07:29:34.458	35.3759	-45.4200	57984.3112	3.21	0.00009	22.00
OMEGA.2017-08-19T07:19:42.536	OMEGA.2017-08-19T07:21:06.796	35.3496	-46.4579	57984.3054	3.14	0.00006	21.75
OMEGA.2017-08-20T07:01:20.698	OMEGA.2017-08-20T07:02:44.928	35.7322	-51.4176	57985.2926	3.49	0.00013	22.02
OMEGA.2017-08-20T06:52:53.706	OMEGA.2017-08-20T06:54:17.946	35.6953	-52.4555	57985.2867	3.46	0.00009	22.15
OMEGA.2017-08-19T07:39:25.470	OMEGA.2017-08-19T07:40:49.830	36.8291	-44.3905	57984.3190	2.92	0.00030	21.62
OMEGA.2017-08-19T07:30:58.708	OMEGA.2017-08-19T07:32:22.899	36.8292	-45.4287	57984.3132	4.85	0.00042	21.97
OMEGA.2017-08-19T07:22:32.747	OMEGA.2017-08-19T07:23:57.037	36.8300	-46.4669	57984.3073	3.12	0.00054	21.51
OMEGA.2017-08-20T07:12:35.169	OMEGA.2017-08-20T07:13:59.410	37.3676	-50.3902	57985.3004	3.83	0.00175	22.23
OMEGA.2017-08-20T07:04:09.248	OMEGA.2017-08-20T07:05:33.538	37.3680	-51.4284	57985.2946	4.09	0.00135	22.20
OMEGA.2017-08-20T06:55:42.597	OMEGA.2017-08-20T06:57:07.256	37.3692	-52.4666	57985.2887	4.21	0.00086	22.15
OMEGA.2017-08-20T05:35:25.813	OMEGA.2017-08-20T05:36:49.923	38.2181	-48.4189	57985.2329	3.38	0.00302	21.85
OMEGA.2017-08-20T05:26:59.982	OMEGA.2017-08-20T05:28:24.272	38.1871	-49.4568	57985.2271	4.72	0.00352	21.93
OMEGA.2017-08-19T07:42:15.890	OMEGA.2017-08-19T07:43:40.010	38.2565	-44.3809	57984.3210	2.86	0.00088	21.92

OMEGA.2017-08-20T05:43:53.614	OMEGA.2017-08-20T05:45:17.834	38.2482	-47.3808	57985.2388	3.70	0.00257	21.96
OMEGA.2017-08-19T07:33:47.429	OMEGA.2017-08-19T07:35:11.509	38.2824	-45.4189	57984.3151	4.07	0.00140	22.00
OMEGA.2017-08-19T07:25:21.318	OMEGA.2017-08-19T07:26:46.058	38.3106	-46.4570	57984.3093	3.08	0.00206	21.71
OMEGA.2017-08-20T07:06:57.759	OMEGA.2017-08-20T07:08:22.349	39.0038	-51.4163	57985.2965	3.19	0.00368	21.93
OMEGA.2017-08-20T06:58:31.717	OMEGA.2017-08-20T06:59:56.457	39.0430	-52.4542	57985.2906	4.84	0.00213	21.97
OMEGA.2017-08-19T06:47:20.771	OMEGA.2017-08-19T06:48:45.061	39.6292	-46.4580	57984.2829	3.47	0.00349	22.06
OMEGA.2017-08-19T07:04:14.453	OMEGA.2017-08-19T07:05:39.094	39.6813	-44.3820	57984.2946	5.29	0.00161	21.99
OMEGA.2017-08-19T06:55:47.382	OMEGA.2017-08-19T06:57:11.642	39.6556	-45.4200	57984.2887	4.36	0.00234	22.06
OMEGA.2017-08-20T05:46:42.045	OMEGA.2017-08-20T05:48:06.265	39.7549	-47.3903	57985.2408	3.34	0.00498	21.57
OMEGA.2017-08-20T05:38:14.005	OMEGA.2017-08-20T05:39:38.333	39.7551	-48.4285	57985.2349	3.00	0.00594	21.93
OMEGA.2017-08-20T05:29:48.812	OMEGA.2017-08-20T05:31:13.042	39.7562	-49.4667	57985.2290	4.29	0.00615	21.93
OMEGA.2017-08-19T09:13:18.786	OMEGA.2017-08-19T09:14:43.076	41.1409	-39.4220	57984.3842	2.93	0.00005	22.08
OMEGA.2017-08-19T09:04:52.424	OMEGA.2017-08-19T09:06:16.915	41.1216	-40.4600	57984.3784	3.15	0.00012	22.01
OMEGA.2017-08-19T08:44:10.010	OMEGA.2017-08-19T08:45:34.091	41.1031	-41.3874	57984.3640	3.52	0.00017	22.16
OMEGA.2017-08-19T08:35:43.649	OMEGA.2017-08-19T08:37:08.160	41.0812	-42.4233	57984.3581	3.51	0.00036	21.68
OMEGA.2017-08-19T08:27:17.828	OMEGA.2017-08-19T08:28:42.088	41.0587	-43.4590	57984.3523	3.38	0.00076	21.85
OMEGA.2017-08-19T07:07:03.424	OMEGA.2017-08-19T07:08:27.655	41.1088	-44.3905	57984.2966	3.47	0.00128	21.83
OMEGA.2017-08-19T06:58:36.133	OMEGA.2017-08-19T07:00:00.413	41.1089	-45.4287	57984.2907	3.25	0.00224	22.11
OMEGA.2017-08-19T06:50:09.302	OMEGA.2017-08-19T06:51:33.542	41.1098	-46.4669	57984.2848	4.59	0.00326	21.96
OMEGA.2017-08-19T09:21:45.707	OMEGA.2017-08-19T09:23:10.058	41.1599	-38.3839	57984.3901	5.26	0.00001	21.98
OMEGA.2017-08-20T05:41:02.704	OMEGA.2017-08-20T05:42:28.834	41.2923	-48.4177	57985.2368	3.54	0.00496	21.88
OMEGA.2017-08-20T05:32:37.272	OMEGA.2017-08-20T05:34:01.573	41.3252	-49.4557	57985.2310	4.08	0.00527	21.81
OMEGA.2017-08-19T09:24:34.918	OMEGA.2017-08-19T09:25:59.178	42.4613	-38.3907	57984.3921	3.71	0.00000	21.84
OMEGA.2017-08-19T09:16:07.316	OMEGA.2017-08-19T09:17:31.687	42.4613	-39.4290	57984.3862	3.17	0.00001	22.07
OMEGA.2017-08-19T09:07:41.135	OMEGA.2017-08-19T09:09:05.385	42.4619	-40.4672	57984.3803	2.96	0.00002	21.92
OMEGA.2017-08-19T08:46:58.441	OMEGA.2017-08-19T08:48:22.661	42.4621	-41.3951	57984.3660	4.47	0.00004	21.73
OMEGA.2017-08-19T08:38:32.750	OMEGA.2017-08-19T08:39:57.360	42.4620	-42.4311	57984.3601	4.93	0.00015	21.84
OMEGA.2017-08-19T08:30:06.739	OMEGA.2017-08-19T08:31:30.989	42.4628	-43.4671	57984.3542	3.36	0.00041	21.68
OMEGA.2017-08-19T07:09:52.665	OMEGA.2017-08-19T07:11:16.925	42.5363	-44.3809	57984.2985	3.61	0.00083	22.06
OMEGA.2017-08-19T07:01:26.033	OMEGA.2017-08-19T07:02:50.283	42.5621	-45.4189	57984.2927	3.69	0.00136	22.33
OMEGA.2017-08-19T06:52:58.522	OMEGA.2017-08-19T06:54:22.982	42.5903	-46.4570	57984.2868	4.11	0.00210	22.27
OMEGA.2017-08-20T06:04:14.838	OMEGA.2017-08-20T06:05:39.068	43.7420	-36.4228	57985.2530	4.11	0.00000	22.04
OMEGA.2017-08-20T05:55:47.967	OMEGA.2017-08-20T05:57:12.607	43.7254	-37.4609	57985.2471	2.96	0.00000	22.12
OMEGA.2017-08-20T06:12:41.169	OMEGA.2017-08-20T06:14:05.420	43.7584	-35.3847	57985.2588	3.54	0.00000	22.26
OMEGA.2017-08-19T09:27:23.458	OMEGA.2017-08-19T09:28:48.438	43.7627	-38.3830	57984.3940	3.61	0.00000	21.79
OMEGA.2017-08-19T09:18:56.467	OMEGA.2017-08-19T09:20:21.447	43.7817	-39.4211	57984.3882	3.51	0.00004	22.00
OMEGA.2017-08-19T09:10:29.605	OMEGA.2017-08-19T09:11:54.125	43.8023	-40.4591	57984.3823	4.41	0.00006	22.15
OMEGA.2017-08-19T08:49:47.421	OMEGA.2017-08-19T08:51:11.732	43.8209	-41.3865	57984.3679	2.95	0.00007	21.68
OMEGA.2017-08-19T08:41:21.720	OMEGA.2017-08-19T08:42:45.921	43.8430	-42.4224	57984.3621	5.08	0.00023	21.97
OMEGA.2017-08-19T08:32:55.308	OMEGA.2017-08-19T08:34:19.549	43.8670	-43.4581	57984.3562	2.96	0.00077	21.78
OMEGA.2017-08-19T08:04:26.774	OMEGA.2017-08-19T08:05:51.434	43.9353	-45.4222	57984.3364	3.74	0.00288	21.80
OMEGA.2017-08-19T07:51:49.322	OMEGA.2017-08-19T07:53:15.503	43.9091	-46.4579	57984.3277	4.42	0.00536	21.60
OMEGA.2017-08-19T08:12:53.805	OMEGA.2017-08-19T08:14:18.086	43.9609	-44.3864	57984.3423	4.10	0.00152	21.46
OMEGA.2017-08-20T06:23:49.231	OMEGA.2017-08-20T06:25:13.471	44.9664	-34.7783	57985.2665	3.21	0.00000	22.17
OMEGA.2017-08-20T06:15:29.950	OMEGA.2017-08-20T06:16:54.160	45.0096	-35.3909	57985.2608	4.10	0.00000	22.11
OMEGA.2017-08-20T06:07:03.968	OMEGA.2017-08-20T06:08:28.269	45.0095	-36.4291	57985.2549	2.97	0.00000	22.20
OMEGA.2017-08-20T05:58:36.837	OMEGA.2017-08-20T06:00:01.347	45.0101	-37.4673	57985.2490	3.75	0.00002	21.83
OMEGA.2017-08-19T08:15:42.336	OMEGA.2017-08-19T08:17:06.926	45.3876	-44.3950	57984.3442	3.39	0.01138	21.25
OMEGA.2017-08-19T08:07:15.755	OMEGA.2017-08-19T08:08:40.154	45.3877	-45.4309	57984.3384	3.10	0.01959	21.98
OMEGA.2017-08-19T07:54:39.802	OMEGA.2017-08-19T07:56:03.902	45.3885	-46.4669	57984.3296	2.90	0.02386	21.92
OMEGA.2017-08-20T06:43:31.634	OMEGA.2017-08-20T06:44:55.865	46.2075	-32.7077	57985.2802	3.66	0.00000	22.19
OMEGA.2017-08-20T06:35:05.883	OMEGA.2017-08-20T06:36:30.103	46.2075	-33.7459	57985.2744	3.79	0.00000	22.07
OMEGA.2017-08-20T06:26:38.312	OMEGA.2017-08-20T06:28:03.822	46.2080	-34.7841	57985.2685	3.63	0.00001	22.12
OMEGA.2017-08-20T07:30:59.112	OMEGA.2017-08-20T07:32:23.173	46.2536	-42.3800	57985.3132	4.09	0.00955	22.45
OMEGA.2017-08-20T07:22:32.911	OMEGA.2017-08-20T07:23:57.472	46.2315	-43.4023	57985.3073	4.16	0.01843	22.24
OMEGA.2017-08-20T06:18:18.240	OMEGA.2017-08-20T06:19:42.890	46.3160	-35.2259	57985.2627	2.86	0.00002	22.06
OMEGA.2017-08-20T06:09:52.639	OMEGA.2017-08-20T06:11:16.879	46.2771	-36.4220	57985.2569	4.02	0.00007	22.25
OMEGA.2017-08-20T07:39:24.944	OMEGA.2017-08-20T07:40:49.174	46.2752	-41.3577	57985.3190	3.88	0.00474	22.07
OMEGA.2017-08-19T08:18:31.216	OMEGA.2017-08-19T08:19:55.547	46.8143	-44.3854	57984.3462	3.19	0.04151	21.29
OMEGA.2017-08-19T08:10:04.394	OMEGA.2017-08-19T08:11:28.905	46.8401	-45.4212	57984.3403	3.64	0.05413	21.64
OMEGA.2017-08-19T08:00:53.974	OMEGA.2017-08-19T08:02:18.483	46.8681	-46.4569	57984.3340	4.58	0.05241	22.20
OMEGA.2017-08-20T08:00:26.557	OMEGA.2017-08-20T08:01:51.048	47.1343	-39.3226	57985.3336	4.34	0.00263	21.78

OMEGA.2017-08-20T07:51:59.766	OMEGA.2017-08-20T07:53:24.016	47.1155	-40.3449	57985.3278	3.10	0.00598	21.97
OMEGA.2017-08-20T06:46:19.945	OMEGA.2017-08-20T06:47:44.305	47.4198	-32.7013	57985.2822	3.22	0.00000	22.11
OMEGA.2017-08-20T06:37:54.383	OMEGA.2017-08-20T06:39:18.723	47.4340	-33.7395	57985.2763	3.01	0.00001	22.26
OMEGA.2017-08-20T06:29:28.052	OMEGA.2017-08-20T06:30:52.572	47.4495	-34.7776	57985.2705	4.28	0.00011	22.00
OMEGA.2017-08-20T07:42:13.674	OMEGA.2017-08-20T07:43:39.285	47.6281	-41.3654	57985.3210	2.85	0.01751	22.16
OMEGA.2017-08-20T07:33:47.523	OMEGA.2017-08-20T07:35:12.343	47.6281	-42.3878	57985.3151	4.07	0.03000	22.20
OMEGA.2017-08-20T07:25:21.932	OMEGA.2017-08-20T07:26:46.152	47.6287	-43.4102	57985.3093	3.69	0.04306	22.33
OMEGA.2017-08-20T08:11:43.089	OMEGA.2017-08-20T08:13:09.690	48.4468	-38.3072	57985.3415	4.48	0.00364	21.82
OMEGA.2017-08-20T08:03:15.878	OMEGA.2017-08-20T08:04:40.109	48.4467	-39.3296	57985.3356	6.02	0.00740	21.86
OMEGA.2017-08-20T07:45:03.365	OMEGA.2017-08-20T07:46:27.595	48.9810	-41.3568	57985.3230	3.67	0.02400	21.86
OMEGA.2017-08-20T07:36:36.493	OMEGA.2017-08-20T07:38:00.614	49.0025	-42.3792	57985.3171	3.39	0.02978	21.62
OMEGA.2017-08-20T07:28:10.702	OMEGA.2017-08-20T07:29:34.992	49.0260	-43.4016	57985.3112	3.12	0.03226	22.24
OMEGA.2017-08-20T08:14:34.020	OMEGA.2017-08-20T08:15:58.250	49.7407	-38.2996	57985.3434	3.10	0.00561	21.89
OMEGA.2017-08-20T08:06:04.488	OMEGA.2017-08-20T08:07:29.579	49.7591	-39.3219	57985.3376	3.20	0.00838	21.75
OMEGA.2017-08-27T09:17:32.910	OMEGA.2017-08-27T09:18:57.091	35.4016	-44.3820	57992.3872	3.41	0.00008	22.07
OMEGA.2017-08-27T09:06:35.988	OMEGA.2017-08-27T09:08:00.248	35.3759	-45.4200	57992.3796	2.91	0.00009	22.16
OMEGA.2017-08-27T08:58:10.627	OMEGA.2017-08-27T08:59:34.707	35.3496	-46.4579	57992.3737	3.09	0.00006	22.12
OMEGA.2017-08-27T08:38:49.184	OMEGA.2017-08-27T08:40:13.684	35.7322	-51.4176	57992.3603	3.63	0.00014	22.24
OMEGA.2017-08-27T08:25:45.831	OMEGA.2017-08-27T08:27:10.071	35.6953	-52.4555	57992.3512	3.24	0.00010	22.18
OMEGA.2017-08-27T09:20:21.431	OMEGA.2017-08-27T09:21:45.701	36.8291	-44.3905	57992.3891	2.92	0.00032	22.30
OMEGA.2017-08-27T09:09:24.579	OMEGA.2017-08-27T09:10:48.829	36.8292	-45.4287	57992.3815	4.50	0.00047	22.04
OMEGA.2017-08-27T09:00:58.958	OMEGA.2017-08-27T09:02:23.218	36.8300	-46.4669	57992.3757	3.11	0.00060	22.04
OMEGA.2017-08-27T08:50:04.306	OMEGA.2017-08-27T08:51:28.566	37.3676	-50.3902	57992.3681	4.67	0.00176	22.10
OMEGA.2017-08-27T08:41:37.914	OMEGA.2017-08-27T08:43:02.424	37.3680	-51.4284	57992.3622	4.18	0.00136	22.12
OMEGA.2017-08-27T08:32:43.573	OMEGA.2017-08-27T08:34:07.793	37.3692	-52.4666	57992.3561	4.04	0.00088	22.18
OMEGA.2017-08-25T08:58:45.676	OMEGA.2017-08-25T09:00:09.906	38.2181	-48.4189	57990.3741	3.90	0.00311	21.81
OMEGA.2017-08-25T08:50:18.975	OMEGA.2017-08-25T08:51:43.324	38.1871	-49.4568	57990.3683	4.29	0.00356	21.96
OMEGA.2017-08-27T09:12:13.389	OMEGA.2017-08-27T09:13:37.460	38.2824	-45.4189	57992.3835	3.57	0.00145	22.01
OMEGA.2017-08-27T09:03:47.468	OMEGA.2017-08-27T09:05:11.628	38.3106	-46.4570	57992.3776	2.98	0.00214	22.02
OMEGA.2017-08-27T08:44:26.654	OMEGA.2017-08-27T08:45:51.165	39.0038	-51.4163	57992.3642	3.20	0.00369	22.28
OMEGA.2017-08-27T08:36:00.663	OMEGA.2017-08-27T08:37:24.923	39.0430	-52.4542	57992.3583	4.67	0.00214	21.96
OMEGA.2017-08-27T08:14:32.069	OMEGA.2017-08-27T08:15:56.589	39.6813	-44.3820	57992.3434	5.13	0.00162	22.26
OMEGA.2017-08-27T08:06:06.368	OMEGA.2017-08-27T08:07:30.609	39.6556	-45.4200	57992.3376	4.48	0.00235	22.23
OMEGA.2017-08-25T09:10:00.698	OMEGA.2017-08-25T09:11:24.938	39.7549	-47.3903	57990.3820	3.25	0.00504	21.93
OMEGA.2017-08-25T09:01:34.416	OMEGA.2017-08-25T09:02:58.916	39.7551	-48.4285	57990.3761	3.53	0.00619	21.90
OMEGA.2017-08-25T08:53:07.605	OMEGA.2017-08-25T08:54:32.495	39.7562	-49.4667	57990.3702	4.38	0.00634	21.72
OMEGA.2017-08-25T08:36:00.522	OMEGA.2017-08-25T08:37:24.782	41.1031	-41.3874	57990.3583	3.54	0.00017	21.90
OMEGA.2017-08-25T08:27:34.521	OMEGA.2017-08-25T08:28:58.610	41.0812	-42.4233	57990.3525	3.60	0.00036	22.23
OMEGA.2017-08-25T08:19:08.689	OMEGA.2017-08-25T08:20:32.989	41.0587	-43.4590	57990.3466	3.27	0.00076	22.05
OMEGA.2017-08-27T08:17:20.840	OMEGA.2017-08-27T08:18:45.501	41.1088	-44.3905	57992.3454	3.30	0.00128	22.28
OMEGA.2017-08-27T08:08:55.128	OMEGA.2017-08-27T08:10:19.359	41.1089	-45.4287	57992.3395	3.22	0.00224	22.41
OMEGA.2017-08-27T08:00:28.647	OMEGA.2017-08-27T08:01:53.357	41.1098	-46.4669	57992.3337	4.59	0.00327	22.41
OMEGA.2017-08-25T09:04:23.057	OMEGA.2017-08-25T09:05:47.317	41.2923	-48.4177	57990.3780	3.27	0.00498	21.98
OMEGA.2017-08-25T08:55:56.895	OMEGA.2017-08-25T08:57:21.415	41.3252	-49.4557	57990.3722	3.58	0.00530	22.06
OMEGA.2017-08-25T08:38:49.053	OMEGA.2017-08-25T08:40:13.143	42.4621	-41.3951	57990.3603	4.52	0.00004	22.03
OMEGA.2017-08-25T08:30:23.141	OMEGA.2017-08-25T08:31:47.382	42.4620	-42.4311	57990.3544	4.90	0.00015	21.90
OMEGA.2017-08-25T08:21:57.350	OMEGA.2017-08-25T08:23:21.450	42.4628	-43.4671	57990.3486	3.35	0.00041	21.98
OMEGA.2017-08-27T08:20:10.300	OMEGA.2017-08-27T08:21:34.811	42.5363	-44.3809	57992.3473	3.69	0.00083	22.27
OMEGA.2017-08-27T08:11:43.538	OMEGA.2017-08-27T08:13:07.810	42.5621	-45.4189	57992.3415	3.70	0.00136	22.23
OMEGA.2017-08-25T09:27:30.801	OMEGA.2017-08-25T09:28:55.041	43.7420	-36.4228	57990.3941	4.06	0.00000	22.04
OMEGA.2017-08-25T09:19:02.919	OMEGA.2017-08-25T09:20:27.160	43.7254	-37.4609	57990.3882	3.03	0.00000	22.02
OMEGA.2017-08-25T08:41:37.493	OMEGA.2017-08-25T08:43:01.713	43.8209	-41.3865	57990.3622	2.99	0.00007	22.04
OMEGA.2017-08-25T08:33:11.742	OMEGA.2017-08-25T08:34:36.003	43.8430	-42.4224	57990.3564	5.04	0.00023	21.94
OMEGA.2017-08-25T08:24:46.050	OMEGA.2017-08-25T08:26:10.441	43.8670	-43.4581	57990.3505	2.96	0.00077	22.04
OMEGA.2017-08-28T09:15:38.735	OMEGA.2017-08-28T09:17:03.046	43.9353	-45.4222	57993.3859	3.45	0.00299	22.43
OMEGA.2017-08-28T09:03:17.823	OMEGA.2017-08-28T09:04:42.063	43.9091	-46.4579	57993.3773	4.41	0.00538	22.47
OMEGA.2017-08-28T09:28:37.418	OMEGA.2017-08-28T09:30:02.013	43.9609	-44.3864	57993.3949	3.67	0.00154	22.43
OMEGA.2017-08-27T06:45:33.874	OMEGA.2017-08-27T06:46:58.115	44.9953	-32.7019	57992.2816	4.26	0.00000	22.38
OMEGA.2017-08-27T06:34:36.432	OMEGA.2017-08-27T06:36:00.813	44.9809	-33.7401	57992.2740	3.77	0.00000	22.04
OMEGA.2017-08-27T06:26:10.131	OMEGA.2017-08-27T06:27:34.521	44.9664	-34.7783	57992.2682	3.35	0.00000	21.98
OMEGA.2017-08-25T09:38:46.333	OMEGA.2017-08-25T09:40:10.673	45.0096	-35.3909	57990.4019	3.16	0.00000	21.80
OMEGA.2017-08-25T09:30:19.291	OMEGA.2017-08-25T09:31:44.101	45.0095	-36.4291	57990.3961	3.52	0.00000	21.97

OMEGA.2017-08-25T09:21:52.020	OMEGA.2017-08-25T09:23:16.540	45.0101	-37.4673	57990.3902	3.32	0.00002	21.91
OMEGA.2017-08-28T09:31:26.238	OMEGA.2017-08-28T09:32:50.469	45.3876	-44.3950	57993.3968	3.90	0.01156	22.45
OMEGA.2017-08-28T09:20:28.326	OMEGA.2017-08-28T09:21:52.557	45.3877	-45.4309	57993.3892	3.11	0.01981	22.40
OMEGA.2017-08-28T09:06:30.214	OMEGA.2017-08-28T09:07:54.914	45.3885	-46.4669	57993.3795	3.08	0.02523	22.45
OMEGA.2017-08-27T06:48:22.435	OMEGA.2017-08-27T06:49:47.355	46.2075	-32.7077	57992.2836	3.85	0.00000	22.35
OMEGA.2017-08-27T06:37:25.133	OMEGA.2017-08-27T06:38:49.553	46.2075	-33.7459	57992.2760	3.76	0.00000	22.10
OMEGA.2017-08-27T06:28:58.942	OMEGA.2017-08-27T06:30:23.662	46.2080	-34.7841	57992.2701	3.62	0.00001	22.19
OMEGA.2017-08-25T07:54:37.965	OMEGA.2017-08-25T07:56:02.515	46.2536	-42.3800	57990.3296	3.76	0.00963	21.80
OMEGA.2017-08-25T07:46:11.614	OMEGA.2017-08-25T07:47:35.854	46.2315	-43.4023	57990.3237	4.30	0.01853	21.91
OMEGA.2017-08-25T09:41:35.443	OMEGA.2017-08-25T09:43:00.023	46.3160	-35.2259	57990.4039	3.13	0.00003	21.89
OMEGA.2017-08-25T09:33:08.472	OMEGA.2017-08-25T09:34:32.722	46.2771	-36.4220	57990.3980	3.07	0.00007	22.03
OMEGA.2017-08-25T08:03:04.706	OMEGA.2017-08-25T08:04:28.957	46.2752	-41.3577	57990.3355	3.75	0.00478	21.98
OMEGA.2017-08-28T09:34:15.288	OMEGA.2017-08-28T09:35:39.749	46.8143	-44.3854	57993.3988	3.79	0.04189	22.44
OMEGA.2017-08-28T09:24:41.777	OMEGA.2017-08-28T09:26:06.037	46.8401	-45.4212	57993.3921	4.51	0.05498	22.46
OMEGA.2017-08-28T09:10:33.225	OMEGA.2017-08-28T09:11:57.535	46.8681	-46.4569	57993.3823	4.25	0.05292	22.46
OMEGA.2017-08-25T07:17:42.409	OMEGA.2017-08-25T07:19:06.649	47.1343	-39.3226	57990.3040	4.51	0.00264	21.84
OMEGA.2017-08-25T07:09:08.747	OMEGA.2017-08-25T07:10:33.028	47.1155	-40.3449	57990.2980	3.38	0.00573	21.66
OMEGA.2017-08-27T06:51:11.606	OMEGA.2017-08-27T06:52:35.865	47.4198	-32.7013	57992.2856	3.10	0.00000	22.37
OMEGA.2017-08-27T06:40:14.064	OMEGA.2017-08-27T06:41:38.354	47.4340	-33.7395	57992.2779	3.04	0.00001	22.06
OMEGA.2017-08-27T06:31:47.922	OMEGA.2017-08-27T06:33:12.212	47.4495	-34.7776	57992.2721	3.84	0.00011	22.08
OMEGA.2017-08-25T08:05:53.467	OMEGA.2017-08-25T08:07:17.712	47.6281	-41.3654	57990.3374	2.95	0.01762	21.88
OMEGA.2017-08-25T07:57:26.816	OMEGA.2017-08-25T07:58:50.906	47.6281	-42.3878	57990.3316	4.13	0.03025	22.00
OMEGA.2017-08-25T07:49:00.244	OMEGA.2017-08-25T07:50:24.304	47.6287	-43.4102	57990.3257	3.64	0.04338	21.86
OMEGA.2017-08-25T07:28:58.061	OMEGA.2017-08-25T07:30:22.391	48.4468	-38.3072	57990.3118	4.64	0.00367	21.83
OMEGA.2017-08-25T07:20:30.919	OMEGA.2017-08-25T07:21:55.179	48.4467	-39.3296	57990.3059	6.20	0.00746	21.85
OMEGA.2017-08-25T08:08:42.327	OMEGA.2017-08-25T08:10:07.997	48.9810	-41.3568	57990.3394	3.89	0.02407	22.01
OMEGA.2017-08-25T08:00:16.376	OMEGA.2017-08-25T08:01:40.466	49.0025	-42.3792	57990.3335	3.41	0.02984	21.89
OMEGA.2017-08-25T07:51:48.385	OMEGA.2017-08-25T07:53:12.725	49.0260	-43.4016	57990.3276	3.10	0.03231	21.93
OMEGA.2017-08-25T07:31:46.631	OMEGA.2017-08-25T07:33:10.902	49.7407	-38.2996	57990.3137	3.04	0.00564	21.92
OMEGA.2017-08-25T07:23:19.440	OMEGA.2017-08-25T07:24:44.590	49.7591	-39.3219	57990.3079	3.26	0.00839	21.59
OMEGA.2017-09-13T07:33:00.155	OMEGA.2017-09-13T07:34:24.395	35.4016	-44.3820	58009.3146	3.38	0.00007	21.64
OMEGA.2017-09-13T07:22:06.953	OMEGA.2017-09-13T07:23:31.324	35.3759	-45.4200	58009.3070	2.89	0.00009	21.65
OMEGA.2017-09-13T07:13:40.812	OMEGA.2017-09-13T07:15:04.912	35.3496	-46.4579	58009.3012	3.03	0.00006	21.75
OMEGA.2017-09-13T06:10:53.211	OMEGA.2017-09-13T06:12:17.441	35.7322	-51.4176	58009.2576	3.25	0.00013	21.96
OMEGA.2017-09-13T06:02:04.120	OMEGA.2017-09-13T06:03:28.360	35.6953	-52.4555	58009.2514	3.22	0.00009	22.06
OMEGA.2017-09-13T06:23:17.063	OMEGA.2017-09-13T06:24:42.103	35.7677	-50.3796	58009.2662	4.32	0.00022	21.83
OMEGA.2017-09-13T07:35:48.906	OMEGA.2017-09-13T07:37:13.306	36.8291	-44.3905	58009.3165	2.85	0.00032	21.81
OMEGA.2017-09-13T07:27:22.474	OMEGA.2017-09-13T07:28:46.694	36.8292	-45.4287	58009.3107	5.08	0.00043	21.75
OMEGA.2017-09-13T07:16:29.752	OMEGA.2017-09-13T07:17:54.012	36.8300	-46.4669	58009.3031	3.05	0.00057	21.82
OMEGA.2017-09-13T06:26:06.174	OMEGA.2017-09-13T06:27:30.414	37.3676	-50.3902	58009.2681	4.54	0.00176	21.88
OMEGA.2017-09-13T06:14:28.722	OMEGA.2017-09-13T06:15:53.082	37.3680	-51.4284	58009.2601	3.94	0.00136	22.07
OMEGA.2017-09-13T06:04:53.400	OMEGA.2017-09-13T06:06:17.930	37.3692	-52.4666	58009.2534	4.35	0.00086	22.02
OMEGA.2017-09-13T04:53:40.038	OMEGA.2017-09-13T04:55:04.258	38.2181	-48.4189	58009.2039	3.30	0.00303	21.94
OMEGA.2017-09-13T04:45:14.376	OMEGA.2017-09-13T04:46:38.736	38.1871	-49.4568	58009.1981	4.53	0.00353	21.57
OMEGA.2017-09-13T07:38:37.586	OMEGA.2017-09-13T07:40:02.086	38.2565	-44.3809	58009.3185	2.80	0.00089	21.81
OMEGA.2017-09-13T05:05:57.210	OMEGA.2017-09-13T05:07:21.500	38.2482	-47.3808	58009.2125	3.67	0.00257	21.68
OMEGA.2017-09-13T07:30:11.025	OMEGA.2017-09-13T07:31:35.505	38.2824	-45.4189	58009.3126	3.46	0.00143	21.73
OMEGA.2017-09-13T07:19:18.142	OMEGA.2017-09-13T07:20:42.482	38.3106	-46.4570	58009.3051	3.01	0.00210	21.75
OMEGA.2017-09-13T06:28:54.704	OMEGA.2017-09-13T06:30:18.744	38.9676	-50.3784	58009.2701	2.89	0.00463	21.93
OMEGA.2017-09-13T06:20:15.772	OMEGA.2017-09-13T06:21:39.863	39.0038	-51.4163	58009.2641	4.14	0.00373	21.90
OMEGA.2017-09-13T06:07:51.430	OMEGA.2017-09-13T06:09:15.720	39.0430	-52.4542	58009.2555	4.75	0.00213	21.80
OMEGA.2017-09-13T06:37:32.375	OMEGA.2017-09-13T06:38:56.646	39.6292	-46.4580	58009.2761	3.27	0.00350	21.77
OMEGA.2017-09-13T06:54:25.078	OMEGA.2017-09-13T06:55:49.299	39.6813	-44.3820	58009.2878	5.02	0.00162	21.89
OMEGA.2017-09-13T06:45:57.606	OMEGA.2017-09-13T06:47:23.067	39.6556	-45.4200	58009.2819	4.69	0.00236	21.74
OMEGA.2017-09-13T05:08:45.701	OMEGA.2017-09-13T05:10:09.921	39.7549	-47.3903	58009.2144	3.27	0.00499	21.81
OMEGA.2017-09-13T04:56:28.969	OMEGA.2017-09-13T04:57:53.178	39.7551	-48.4285	58009.2059	3.05	0.00594	21.82
OMEGA.2017-09-13T04:48:02.957	OMEGA.2017-09-13T04:49:27.177	39.7562	-49.4667	58009.2000	4.22	0.00617	21.75
OMEGA.2017-09-12T08:40:57.399	OMEGA.2017-09-12T08:42:21.479	41.1409	-39.4220	58008.3618	2.94	0.00005	21.74
OMEGA.2017-09-12T08:32:32.138	OMEGA.2017-09-12T08:33:56.328	41.1216	-40.4600	58008.3559	3.08	0.00012	21.55
OMEGA.2017-09-15T05:28:06.952	OMEGA.2017-09-15T05:29:31.302	41.1031	-41.3874	58011.2279	3.54	0.00017	22.28
OMEGA.2017-09-15T05:15:04.159	OMEGA.2017-09-15T05:16:28.220	41.0812	-42.4233	58011.2188	3.43	0.00036	22.21
OMEGA.2017-09-15T05:06:37.218	OMEGA.2017-09-15T05:08:01.278	41.0587	-43.4590	58011.2129	3.42	0.00076	22.33

OMEGA.2017-09-13T07:00:51.909	OMEGA.2017-09-13T07:02:16.130	41.1088	-44.3905	58009.2923	3.14	0.00129	21.84
OMEGA.2017-09-13T06:48:47.287	OMEGA.2017-09-13T06:50:12.137	41.1089	-45.4287	58009.2839	3.21	0.00224	21.87
OMEGA.2017-09-13T06:40:21.126	OMEGA.2017-09-13T06:41:45.186	41.1098	-46.4669	58009.2780	4.45	0.00328	21.93
OMEGA.2017-09-12T08:49:23.300	OMEGA.2017-09-12T08:50:47.531	41.1599	-38.3839	58008.3676	4.84	0.00001	21.42
OMEGA.2017-09-13T05:03:05.509	OMEGA.2017-09-13T05:04:29.740	41.2923	-48.4177	58009.2105	3.37	0.00500	21.75
OMEGA.2017-09-13T04:50:51.237	OMEGA.2017-09-13T04:52:15.747	41.3252	-49.4557	58009.2020	3.86	0.00527	21.74
OMEGA.2017-09-12T08:52:11.861	OMEGA.2017-09-12T08:53:35.921	42.4613	-38.3907	58008.3696	3.18	0.00000	21.19
OMEGA.2017-09-12T08:43:45.749	OMEGA.2017-09-12T08:45:10.240	42.4613	-39.4290	58008.3637	3.48	0.00001	21.59
OMEGA.2017-09-12T08:35:20.558	OMEGA.2017-09-12T08:36:44.789	42.4619	-40.4672	58008.3579	3.63	0.00003	21.87
OMEGA.2017-09-15T05:30:55.532	OMEGA.2017-09-15T05:32:19.632	42.4621	-41.3951	58011.2298	4.43	0.00004	22.22
OMEGA.2017-09-15T05:17:53.320	OMEGA.2017-09-15T05:19:17.710	42.4620	-42.4311	58011.2208	4.69	0.00015	22.24
OMEGA.2017-09-15T05:09:25.869	OMEGA.2017-09-15T05:10:49.978	42.4628	-43.4671	58011.2149	3.32	0.00041	22.33
OMEGA.2017-09-13T07:06:16.321	OMEGA.2017-09-13T07:07:40.790	42.5363	-44.3809	58009.2960	3.85	0.00083	21.78
OMEGA.2017-09-13T06:51:36.568	OMEGA.2017-09-13T06:53:00.778	42.5621	-45.4189	58009.2858	3.40	0.00137	21.85
OMEGA.2017-09-12T09:13:03.275	OMEGA.2017-09-12T09:14:27.655	43.7420	-36.4228	58008.3841	4.37	0.00000	21.52
OMEGA.2017-09-12T09:04:37.743	OMEGA.2017-09-12T09:06:01.943	43.7254	-37.4609	58008.3782	2.99	0.00000	21.50
OMEGA.2017-09-12T09:21:29.656	OMEGA.2017-09-12T09:22:53.796	43.7584	-35.3847	58008.3899	4.54	0.00000	21.44
OMEGA.2017-09-12T08:55:00.261	OMEGA.2017-09-12T08:56:24.622	43.7627	-38.3830	58008.3715	3.48	0.00001	21.18
OMEGA.2017-09-12T08:46:34.470	OMEGA.2017-09-12T08:47:58.720	43.7817	-39.4211	58008.3657	3.96	0.00004	21.51
OMEGA.2017-09-12T08:38:09.018	OMEGA.2017-09-12T08:39:33.319	43.8023	-40.4591	58008.3598	4.36	0.00007	21.53
OMEGA.2017-09-15T05:33:44.383	OMEGA.2017-09-15T05:35:08.683	43.8209	-41.3865	58011.2318	3.09	0.00007	22.20
OMEGA.2017-09-15T05:25:03.881	OMEGA.2017-09-15T05:26:28.242	43.8430	-42.4224	58011.2257	3.67	0.00024	22.37
OMEGA.2017-09-15T05:12:15.679	OMEGA.2017-09-15T05:13:39.929	43.8670	-43.4581	58011.2168	2.95	0.00077	22.41
OMEGA.2017-09-15T04:40:12.204	OMEGA.2017-09-15T04:41:36.693	43.9353	-45.4222	58011.1946	3.61	0.00287	22.14
OMEGA.2017-09-15T04:31:36.472	OMEGA.2017-09-15T04:33:00.702	43.9091	-46.4579	58011.1886	4.03	0.00529	22.09
OMEGA.2017-09-15T04:52:13.007	OMEGA.2017-09-15T04:53:37.415	43.9609	-44.3864	58011.2029	3.72	0.00152	22.38
OMEGA.2017-09-13T05:46:24.157	OMEGA.2017-09-13T05:47:48.407	44.9953	-32.7019	58009.2406	4.05	0.00000	21.78
OMEGA.2017-09-13T05:33:53.554	OMEGA.2017-09-13T05:35:17.745	44.9809	-33.7401	58009.2319	3.63	0.00000	21.67
OMEGA.2017-09-13T05:24:58.413	OMEGA.2017-09-13T05:26:22.633	44.9664	-34.7783	58009.2257	3.22	0.00000	21.76
OMEGA.2017-09-12T09:24:18.296	OMEGA.2017-09-12T09:25:42.807	45.0096	-35.3909	58008.3919	2.89	0.00000	21.17
OMEGA.2017-09-12T09:15:52.265	OMEGA.2017-09-12T09:17:16.595	45.0095	-36.4291	58008.3860	3.46	0.00000	21.40
OMEGA.2017-09-12T09:07:26.033	OMEGA.2017-09-12T09:08:50.244	45.0101	-37.4673	58008.3802	3.23	0.00002	21.70
OMEGA.2017-09-15T04:55:01.646	OMEGA.2017-09-15T04:56:28.266	45.3876	-44.3950	58011.2049	3.52	0.01140	22.19
OMEGA.2017-09-15T04:45:26.564	OMEGA.2017-09-15T04:46:50.805	45.3877	-45.4309	58011.1982	3.13	0.01980	22.32
OMEGA.2017-09-15T04:34:24.992	OMEGA.2017-09-15T04:35:49.083	45.3885	-46.4669	58011.1906	2.89	0.02396	22.21
OMEGA.2017-09-13T05:49:12.887	OMEGA.2017-09-13T05:50:37.138	46.2075	-32.7077	58009.2425	3.55	0.00000	21.66
OMEGA.2017-09-13T05:36:42.125	OMEGA.2017-09-13T05:38:06.365	46.2075	-33.7459	58009.2338	3.68	0.00000	21.89
OMEGA.2017-09-13T05:28:10.104	OMEGA.2017-09-13T05:29:34.314	46.2080	-34.7841	58009.2279	3.58	0.00001	21.68
OMEGA.2017-09-12T07:24:03.746	OMEGA.2017-09-12T07:25:28.726	46.2536	-42.3800	58008.3084	3.64	0.00969	21.32
OMEGA.2017-09-12T07:15:38.275	OMEGA.2017-09-12T07:17:02.505	46.2315	-43.4023	58008.3025	4.20	0.01853	21.49
OMEGA.2017-09-12T09:27:07.187	OMEGA.2017-09-12T09:28:31.828	46.3160	-35.2259	58008.3938	2.97	0.00003	21.17
OMEGA.2017-09-12T09:18:41.025	OMEGA.2017-09-12T09:20:05.265	46.2771	-36.4220	58008.3880	3.04	0.00008	21.43
OMEGA.2017-09-12T07:32:32.607	OMEGA.2017-09-12T07:33:56.917	46.2752	-41.3577	58008.3143	3.69	0.00482	21.51
OMEGA.2017-09-12T09:10:14.774	OMEGA.2017-09-12T09:11:39.005	46.2949	-37.4602	58008.3821	3.56	0.00020	21.39
OMEGA.2017-09-15T04:57:52.506	OMEGA.2017-09-15T04:59:16.787	46.8143	-44.3854	58011.2069	3.29	0.04151	22.32
OMEGA.2017-09-15T04:49:24.535	OMEGA.2017-09-15T04:50:48.775	46.8401	-45.4212	58011.2010	3.66	0.05424	21.62
OMEGA.2017-09-15T04:37:13.213	OMEGA.2017-09-15T04:38:37.473	46.8681	-46.4569	58011.1925	4.41	0.05249	22.10
OMEGA.2017-09-12T08:01:39.303	OMEGA.2017-09-12T08:03:03.383	47.1343	-39.3226	58008.3345	4.80	0.00270	21.46
OMEGA.2017-09-12T07:53:13.461	OMEGA.2017-09-12T07:54:37.701	47.1155	-40.3449	58008.3286	2.89	0.00604	21.58
OMEGA.2017-09-12T08:10:04.384	OMEGA.2017-09-12T08:11:28.544	47.1529	-38.3003	58008.3403	2.88	0.00114	21.46
OMEGA.2017-09-13T05:52:01.277	OMEGA.2017-09-13T05:53:25.508	47.4198	-32.7013	58009.2445	3.09	0.00000	21.58
OMEGA.2017-09-13T05:39:30.606	OMEGA.2017-09-13T05:40:54.876	47.4340	-33.7395	58009.2358	2.92	0.00001	21.65
OMEGA.2017-09-13T05:30:59.114	OMEGA.2017-09-13T05:32:23.324	47.4495	-34.7776	58009.2299	3.76	0.00011	21.48
OMEGA.2017-09-12T07:35:21.138	OMEGA.2017-09-12T07:36:45.798	47.6281	-41.3654	58008.3162	2.92	0.01776	21.50
OMEGA.2017-09-12T07:26:55.037	OMEGA.2017-09-12T07:28:19.316	47.6281	-42.3878	58008.3104	4.25	0.03045	21.45
OMEGA.2017-09-12T07:18:26.725	OMEGA.2017-09-12T07:19:51.036	47.6287	-43.4102	58008.3045	3.62	0.04358	21.45
OMEGA.2017-09-12T08:12:52.764	OMEGA.2017-09-12T08:14:16.835	48.4468	-38.3072	58008.3423	4.99	0.00378	21.67
OMEGA.2017-09-12T08:04:27.603	OMEGA.2017-09-12T08:05:51.823	48.4467	-39.3296	58008.3364	5.91	0.00764	21.63
OMEGA.2017-09-12T07:56:01.931	OMEGA.2017-09-12T07:57:26.812	48.4472	-40.3521	58008.3306	3.87	0.01412	21.47
OMEGA.2017-09-12T07:38:10.018	OMEGA.2017-09-12T07:39:34.319	48.9810	-41.3568	58008.3182	4.04	0.02417	21.50
OMEGA.2017-09-12T07:29:43.547	OMEGA.2017-09-12T07:31:08.037	49.0025	-42.3792	58008.3123	3.28	0.02991	21.43
OMEGA.2017-09-12T07:21:15.265	OMEGA.2017-09-12T07:22:39.526	49.0260	-43.4016	58008.3064	3.01	0.03236	21.21

OMEGA.2017-09-12T08:15:40.935	OMEGA.2017-09-12T08:17:05.194	49.7407	-38.2996	58008.3442	3.00	0.00569	21.87
OMEGA.2017-09-12T08:07:16.143	OMEGA.2017-09-12T08:08:40.324	49.7591	-39.3219	58008.3384	3.47	0.00856	21.64
OMEGA.2017-09-12T07:58:51.042	OMEGA.2017-09-12T08:00:15.122	49.7791	-40.3443	58008.3325	3.45	0.01277	21.35
OMEGA.2017-09-29T02:40:19.113	OMEGA.2017-09-29T02:41:43.743	35.4016	-44.3820	58025.1113	3.90	0.00007	22.08
OMEGA.2017-09-29T02:31:53.591	OMEGA.2017-09-29T02:33:17.811	35.3759	-45.4200	58025.1055	3.13	0.00009	21.99
OMEGA.2017-09-29T02:23:26.670	OMEGA.2017-09-29T02:24:50.910	35.3496	-46.4579	58025.0996	3.10	0.00006	21.96
OMEGA.2017-09-28T08:53:41.861	OMEGA.2017-09-28T08:55:05.941	35.7322	-51.4176	58024.3706	3.40	0.00015	22.19
OMEGA.2017-09-28T08:45:16.549	OMEGA.2017-09-28T08:46:40.790	35.6953	-52.4555	58024.3648	3.36	0.00010	22.23
OMEGA.2017-09-28T09:02:07.292	OMEGA.2017-09-28T09:03:31.952	35.7677	-50.3796	58024.3765	5.02	0.00023	22.10
OMEGA.2017-09-29T02:43:08.053	OMEGA.2017-09-29T02:44:32.314	36.8291	-44.3905	58025.1133	2.98	0.00031	22.06
OMEGA.2017-09-29T02:34:42.092	OMEGA.2017-09-29T02:36:06.262	36.8292	-45.4287	58025.1074	5.05	0.00042	21.93
OMEGA.2017-09-29T02:26:15.220	OMEGA.2017-09-29T02:27:39.481	36.8300	-46.4669	58025.1016	3.07	0.00054	21.96
OMEGA.2017-09-28T09:04:56.283	OMEGA.2017-09-28T09:06:20.353	37.3676	-50.3902	58024.3784	6.44	0.00189	22.24
OMEGA.2017-09-28T08:56:30.101	OMEGA.2017-09-28T08:57:54.322	37.3680	-51.4284	58024.3726	4.80	0.00151	22.30
OMEGA.2017-09-28T08:48:05.100	OMEGA.2017-09-28T08:49:29.330	37.3692	-52.4666	58024.3667	3.12	0.00095	22.20
OMEGA.2017-09-28T03:57:11.280	OMEGA.2017-09-28T03:58:36.070	38.2181	-48.4189	58024.1647	3.53	0.00301	22.03
OMEGA.2017-09-28T03:48:44.478	OMEGA.2017-09-28T03:50:09.518	38.1871	-49.4568	58024.1588	4.62	0.00354	21.83
OMEGA.2017-09-29T02:45:56.634	OMEGA.2017-09-29T02:47:20.864	38.2565	-44.3809	58025.1152	2.89	0.00088	21.97
OMEGA.2017-09-28T04:05:37.901	OMEGA.2017-09-28T04:07:02.832	38.2482	-47.3808	58024.1706	3.57	0.00257	22.17
OMEGA.2017-09-29T02:37:30.532	OMEGA.2017-09-29T02:38:54.863	38.2824	-45.4189	58025.1094	3.87	0.00140	22.01
OMEGA.2017-09-29T02:29:05.011	OMEGA.2017-09-29T02:30:29.491	38.3106	-46.4570	58025.1035	3.66	0.00207	21.85
OMEGA.2017-09-28T09:07:44.443	OMEGA.2017-09-28T09:09:08.543	38.9676	-50.3784	58024.3804	3.18	0.00475	22.22
OMEGA.2017-09-28T08:59:18.582	OMEGA.2017-09-28T09:00:42.942	39.0038	-51.4163	58024.3745	4.38	0.00379	22.11
OMEGA.2017-09-28T08:50:53.580	OMEGA.2017-09-28T08:52:17.770	39.0430	-52.4542	58024.3687	3.72	0.00218	22.13
OMEGA.2017-09-29T01:52:27.665	OMEGA.2017-09-29T01:53:51.895	39.6292	-46.4580	58025.0781	3.61	0.00347	21.77
OMEGA.2017-09-29T02:09:21.668	OMEGA.2017-09-29T02:10:45.768	39.6813	-44.3820	58025.0898	5.41	0.00161	21.92
OMEGA.2017-09-29T02:00:54.466	OMEGA.2017-09-29T02:02:18.697	39.6556	-45.4200	58025.0840	4.39	0.00233	21.91
OMEGA.2017-09-28T04:08:27.062	OMEGA.2017-09-28T04:09:51.562	39.7549	-47.3903	58024.1725	3.51	0.00497	22.07
OMEGA.2017-09-28T04:00:00.280	OMEGA.2017-09-28T04:01:24.511	39.7551	-48.4285	58024.1667	3.17	0.00594	22.17
OMEGA.2017-09-28T03:51:33.920	OMEGA.2017-09-28T03:52:58.279	39.7562	-49.4667	58024.1608	4.24	0.00610	21.96
OMEGA.2017-09-28T03:24:57.204	OMEGA.2017-09-28T03:26:21.824	41.1409	-39.4220	58024.1423	2.98	0.00005	21.70
OMEGA.2017-09-28T03:16:31.303	OMEGA.2017-09-28T03:17:55.553	41.1216	-40.4600	58024.1365	3.19	0.00012	21.95
OMEGA.2017-09-29T04:03:14.987	OMEGA.2017-09-29T04:04:39.077	41.1031	-41.3874	58025.1689	3.53	0.00017	22.15
OMEGA.2017-09-29T03:54:49.245	OMEGA.2017-09-29T03:56:13.496	41.0812	-42.4233	58025.1631	3.53	0.00036	22.16
OMEGA.2017-09-29T03:46:23.364	OMEGA.2017-09-29T03:47:47.645	41.0587	-43.4590	58025.1572	3.48	0.00076	22.23
OMEGA.2017-09-29T02:12:10.248	OMEGA.2017-09-29T02:13:34.468	41.1088	-44.3905	58025.0918	3.53	0.00128	21.93
OMEGA.2017-09-29T02:03:43.757	OMEGA.2017-09-29T02:05:08.137	41.1089	-45.4287	58025.0859	3.12	0.00223	21.94
OMEGA.2017-09-29T01:55:16.775	OMEGA.2017-09-29T01:56:41.155	41.1098	-46.4669	58025.0801	4.39	0.00325	21.88
OMEGA.2017-09-28T03:33:23.886	OMEGA.2017-09-28T03:34:48.076	41.1599	-38.3839	58024.1482	3.79	0.00001	21.90
OMEGA.2017-09-28T04:11:16.082	OMEGA.2017-09-28T04:12:40.903	41.2616	-47.3798	58024.1745	3.68	0.00411	22.03
OMEGA.2017-09-28T04:02:49.111	OMEGA.2017-09-28T04:04:13.531	41.2923	-48.4177	58024.1686	3.57	0.00496	22.02
OMEGA.2017-09-28T03:54:22.679	OMEGA.2017-09-28T03:55:47.019	41.3252	-49.4557	58024.1628	3.71	0.00527	21.88
OMEGA.2017-09-28T03:36:12.696	OMEGA.2017-09-28T03:37:36.926	42.4613	-38.3907	58024.1501	3.49	0.00000	21.91
OMEGA.2017-09-28T03:27:46.535	OMEGA.2017-09-28T03:29:10.615	42.4613	-39.4290	58024.1443	3.04	0.00001	21.83
OMEGA.2017-09-28T03:19:19.793	OMEGA.2017-09-28T03:20:44.034	42.4619	-40.4672	58024.1384	2.95	0.00002	21.91
OMEGA.2017-09-29T04:06:03.597	OMEGA.2017-09-29T04:07:27.738	42.4621	-41.3951	58025.1709	4.43	0.00004	22.13
OMEGA.2017-09-29T03:57:37.816	OMEGA.2017-09-29T03:59:02.027	42.4620	-42.4311	58025.1650	4.58	0.00015	22.12
OMEGA.2017-09-29T03:49:11.904	OMEGA.2017-09-29T03:50:36.135	42.4628	-43.4671	58025.1592	3.57	0.00041	22.35
OMEGA.2017-09-29T02:14:58.739	OMEGA.2017-09-29T02:16:23.059	42.5363	-44.3809	58025.0937	3.60	0.00083	21.63
OMEGA.2017-09-29T02:06:32.757	OMEGA.2017-09-29T02:07:57.357	42.5621	-45.4189	58025.0879	3.71	0.00136	21.78
OMEGA.2017-09-29T01:58:05.395	OMEGA.2017-09-29T01:59:30.246	42.5903	-46.4570	58025.0820	3.98	0.00210	21.61
OMEGA.2017-09-28T04:30:16.146	OMEGA.2017-09-28T04:31:40.586	43.7420	-36.4228	58024.1877	3.80	0.00000	22.09
OMEGA.2017-09-28T04:21:49.554	OMEGA.2017-09-28T04:23:14.044	43.7254	-37.4609	58024.1818	2.94	0.00000	22.04
OMEGA.2017-09-28T04:38:42.367	OMEGA.2017-09-28T04:40:06.867	43.7584	-35.3847	58024.1935	3.44	0.00000	22.43
OMEGA.2017-09-28T03:39:01.316	OMEGA.2017-09-28T03:40:25.577	43.7627	-38.3830	58024.1521	3.61	0.00000	21.58
OMEGA.2017-09-28T03:30:34.955	OMEGA.2017-09-28T03:31:59.635	43.7817	-39.4211	58024.1462	3.20	0.00004	21.54
OMEGA.2017-09-28T03:22:08.543	OMEGA.2017-09-28T03:23:32.884	43.8023	-40.4591	58024.1404	4.09	0.00006	21.69
OMEGA.2017-09-29T04:08:51.898	OMEGA.2017-09-29T04:10:16.148	43.8209	-41.3865	58025.1728	3.04	0.00007	22.07
OMEGA.2017-09-29T04:00:26.256	OMEGA.2017-09-29T04:01:50.877	43.8430	-42.4224	58025.1670	4.83	0.00023	22.10
OMEGA.2017-09-29T03:52:00.755	OMEGA.2017-09-29T03:53:24.946	43.8670	-43.4581	58025.1611	3.03	0.00076	22.04
OMEGA.2017-09-29T03:25:23.540	OMEGA.2017-09-29T03:26:47.911	43.9353	-45.4222	58025.1426	3.62	0.00286	22.07
OMEGA.2017-09-29T03:16:56.689	OMEGA.2017-09-29T03:18:20.969	43.9091	-46.4579	58025.1368	4.03	0.00527	22.05

OMEGA.2017-09-29T03:33:49.052	OMEGA.2017-09-29T03:35:13.342	43.9609	-44.3864	58025.1485	3.87	0.00152	22.04
OMEGA.2017-09-28T08:30:35.457	OMEGA.2017-09-28T08:31:59.847	44.9953	-32.7019	58024.3546	4.32	0.00000	22.30
OMEGA.2017-09-28T08:22:09.185	OMEGA.2017-09-28T08:23:33.665	44.9809	-33.7401	58024.3487	3.05	0.00000	22.35
OMEGA.2017-09-28T08:13:43.413	OMEGA.2017-09-28T08:15:07.654	44.9664	-34.7783	58024.3429	3.25	0.00000	22.14
OMEGA.2017-09-28T04:44:20.788	OMEGA.2017-09-28T04:45:44.888	45.0096	-35.3909	58024.1975	3.97	0.00000	22.19
OMEGA.2017-09-28T04:33:04.836	OMEGA.2017-09-28T04:34:29.166	45.0095	-36.4291	58024.1896	3.09	0.00000	22.29
OMEGA.2017-09-28T04:24:38.324	OMEGA.2017-09-28T04:26:02.565	45.0101	-37.4673	58024.1838	3.67	0.00002	22.07
OMEGA.2017-09-29T03:36:37.582	OMEGA.2017-09-29T03:38:01.913	45.3876	-44.3950	58025.1504	3.54	0.01136	22.08
OMEGA.2017-09-29T03:28:12.281	OMEGA.2017-09-29T03:29:36.351	45.3877	-45.4309	58025.1446	3.14	0.01957	22.01
OMEGA.2017-09-29T03:19:45.209	OMEGA.2017-09-29T03:21:09.450	45.3885	-46.4669	58025.1387	2.94	0.02373	21.98
OMEGA.2017-09-28T08:33:25.797	OMEGA.2017-09-28T08:34:50.308	46.2075	-32.7077	58024.3565	4.44	0.00000	22.08
OMEGA.2017-09-28T08:24:57.896	OMEGA.2017-09-28T08:26:22.086	46.2075	-33.7459	58024.3507	4.00	0.00000	22.26
OMEGA.2017-09-28T08:16:31.924	OMEGA.2017-09-28T08:17:56.094	46.2080	-34.7841	58024.3448	3.74	0.00001	22.13
OMEGA.2017-09-28T07:23:25.007	OMEGA.2017-09-28T07:24:49.735	46.2536	-42.3800	58024.3079	3.99	0.01017	22.17
OMEGA.2017-09-28T07:14:59.584	OMEGA.2017-09-28T07:16:23.684	46.2315	-43.4023	58024.3021	4.03	0.01879	22.19
OMEGA.2017-09-28T04:35:53.906	OMEGA.2017-09-28T04:37:18.116	46.2771	-36.4220	58024.1916	3.69	0.00007	22.37
OMEGA.2017-09-28T07:31:51.317	OMEGA.2017-09-28T07:33:17.657	46.2752	-41.3577	58024.3138	3.96	0.00510	22.29
OMEGA.2017-09-28T04:27:26.805	OMEGA.2017-09-28T04:28:51.265	46.2949	-37.4602	58024.1857	4.24	0.00019	21.93
OMEGA.2017-09-29T03:39:26.163	OMEGA.2017-09-29T03:40:50.443	46.8143	-44.3854	58025.1524	3.35	0.04145	22.11
OMEGA.2017-09-29T03:31:00.582	OMEGA.2017-09-29T03:32:24.912	46.8401	-45.4212	58025.1465	3.51	0.05415	21.88
OMEGA.2017-09-29T03:22:34.780	OMEGA.2017-09-29T03:23:59.010	46.8681	-46.4569	58025.1407	4.43	0.05241	21.94
OMEGA.2017-09-28T07:52:20.150	OMEGA.2017-09-28T07:53:44.380	47.1343	-39.3226	58024.3280	3.96	0.00281	21.87
OMEGA.2017-09-28T07:43:48.268	OMEGA.2017-09-28T07:45:12.499	47.1155	-40.3449	58024.3221	2.96	0.00604	22.21
OMEGA.2017-09-28T08:00:46.181	OMEGA.2017-09-28T08:02:10.421	47.1529	-38.3003	58024.3339	2.92	0.00119	21.92
OMEGA.2017-09-28T08:36:14.528	OMEGA.2017-09-28T08:37:38.958	47.4198	-32.7013	58024.3585	3.38	0.00000	22.12
OMEGA.2017-09-28T08:27:46.826	OMEGA.2017-09-28T08:29:11.177	47.4340	-33.7395	58024.3526	3.03	0.00001	22.01
OMEGA.2017-09-28T08:19:20.684	OMEGA.2017-09-28T08:20:44.935	47.4495	-34.7776	58024.3468	3.54	0.00012	22.06
OMEGA.2017-09-28T07:34:41.917	OMEGA.2017-09-28T07:36:06.417	47.6281	-41.3654	58024.3158	2.87	0.01902	22.01
OMEGA.2017-09-28T07:26:14.076	OMEGA.2017-09-28T07:27:38.596	47.6281	-42.3878	58024.3099	4.90	0.03232	22.23
OMEGA.2017-09-28T07:17:47.774	OMEGA.2017-09-28T07:19:12.365	47.6287	-43.4102	58024.3040	4.58	0.04553	22.12
OMEGA.2017-09-28T08:03:34.832	OMEGA.2017-09-28T08:04:59.092	48.4468	-38.3072	58024.3358	4.70	0.00398	21.93
OMEGA.2017-09-28T07:55:08.521	OMEGA.2017-09-28T07:56:33.091	48.4467	-39.3296	58024.3300	5.14	0.00797	21.84
OMEGA.2017-09-28T07:46:36.799	OMEGA.2017-09-28T07:48:01.090	48.4472	-40.3521	58024.3240	4.30	0.01465	21.97
OMEGA.2017-09-28T07:37:30.668	OMEGA.2017-09-28T07:38:54.988	48.9810	-41.3568	58024.3177	4.62	0.02448	21.98
OMEGA.2017-09-28T07:29:02.926	OMEGA.2017-09-28T07:30:27.086	49.0025	-42.3792	58024.3118	4.06	0.03006	22.14
OMEGA.2017-09-28T07:20:36.595	OMEGA.2017-09-28T07:22:00.825	49.0260	-43.4016	58024.3060	3.61	0.03242	22.06
OMEGA.2017-09-28T08:06:23.323	OMEGA.2017-09-28T08:07:47.583	49.7407	-38.2996	58024.3378	3.06	0.00574	21.92
OMEGA.2017-09-28T07:57:57.581	OMEGA.2017-09-28T07:59:21.832	49.7591	-39.3219	58024.3319	4.04	0.00864	21.93
OMEGA.2017-09-28T07:49:25.349	OMEGA.2017-09-28T07:50:49.670	49.7791	-40.3443	58024.3260	4.38	0.01283	22.02

REFERENCES

- Aasi J., et al., 2015, *Classical and Quantum Gravity*, **32**, 115012
- Abbott B. P., et al., 2017a, *Physical Review Letters*, **119**, 141101
- Abbott B. P., et al., 2017b, *Physical Review Letters*, **119**, 161101
- Acernese F., et al., 2015, *Classical and Quantum Gravity*, **32**, 024001
- Alam S., et al., 2015, *ApJS*, **219**, 12
- Bartos I., 2016, in American Astronomical Society Meeting Abstracts #228. p. 208.03
- Becker A., 2015, HOTPANTS: High Order Transform of PSF ANd Template Subtraction, Astrophysics Source Code Library (ascl:1504.004)
- Berthier J., Vachier F., Thuillot W., Fernique P., Ochsenbein F., Genova F., Lainey V., Arlot J.-E., 2006, in Gabriel C., Arviset C., Ponz D., Enrique S., eds, *Astronomical Society of the Pacific Conference Series Vol. 351, Astronomical Data Analysis Software and Systems XV*. p. 367
- Bertin E., 2006, in Gabriel C., Arviset C., Ponz D., Enrique S., eds, *Astronomical Society of the Pacific Conference Series Vol. 351, Astronomical Data Analysis Software and Systems XV*. p. 112
- Bertin E., 2009, *Mem. Soc. Astron. Italiana*, **80**, 422
- Brocato E., et al., 2018, *MNRAS*, **474**, 411
- Capaccioli M., Mancini D., Sedmak G., 2003, *Mem. Soc. Astron. Italiana*, **74**, 450
- Capaccioli M., et al., 2015, *A&A*, **581**, A10
- Cappellaro E., et al., 2015, *A&A*, **584**, A62
- Dályá G., et al., 2018, *MNRAS*, **479**, 2374
- Delgado A., Harrison D., Hodgkin S., Leeuwen M. V., Rixon G., Yoldas A., 2017, *Transient Name Server Discovery Report*, **632**
- Doctor Z., et al., 2019, *ApJ*, **873**, L24
- Doi M., et al., 2010, *AJ*, **139**, 1628
- Grado A., Capaccioli M., Limatola L., Getman F., 2012, *Memorie della Societa Astronomica Italiana Supplementi*, **19**, 362
- Greco G., Grado A., Getman F., Cappellaro E., Branchesi M., Covino S., GRAWITA-GRavitational Wave Inaf TeAm 2017, GRB Coordinates Network, Circular Service, No. 21498, #1 (2017), 21498
- Hastie T., Tibshirani R., 1986, *Statist. Sci.*, **1**, 297
- Høg E., et al., 2000, *A&A*, **355**, L27
- Kalogera V., Belczynski K., Kim C., O'Shaughnessy R., Willems B., 2007, *Phys. Rep.*, **442**, 75
- Kuijken K., 2011, *The Messenger*, **146**, 8
- Mieske S., 2018, in *VST in the Era of the Large Sky Surveys*. p. 5, doi:10.5281/zenodo.1303284
- Miller A. A., et al., 2009, *ApJ*, **690**, 1303
- Murase K., Kashiyama K., Mészáros P., Shoemaker I., Senno N., 2016, *ApJ*, **822**, L9
- Pankow C., Sampson L., Perri L., Chase E., Coughlin S., Zevin M., Kalogera V., 2017, *ApJ*, **834**, 154
- Perna R., Lazzati D., Giacomazzo B., 2016, *ApJ*, **821**, L18
- Perna R., Chruslinska M., Corsi A., Belczynski K., 2018, *MNRAS*, **477**, 4228
- Perna R., Lazzati D., Farr W., 2019, *ApJ*, **875**, 49
- Pian E., et al., 2017, *Nature*, **551**, 67
- Planck Collaboration et al., 2016, *A&A*, **594**, A13
- Radovich M., et al., 2004, *A&A*, **417**, 51
- Rodriguez C. L., Chatterjee S., Rasio F. A., 2016, *Phys. Rev. D*, **93**, 084029
- Schutz B. F., 1986, *Nature*, **323**, 310
- Singer L. P., Price L. R., 2016, *Phys. Rev. D*, **93**, 024013
- Skrutskie M. F., et al., 2006, *AJ*, **131**, 1163
- Stone N. C., Metzger B. D., Haiman Z., 2017, *MNRAS*, **464**, 946
- Strader J., Chomiuk L., Tremou E. e. a., 2017, *Transient Name Server Classification Report*, **833**
- The LIGO Scientific Collaboration the Virgo Collaboration 2017a, GRB Coordinates Network, Circular Service, No. 21474, #1 (2017a), 21474
- The LIGO Scientific Collaboration the Virgo Collaboration 2017b, GRB Coordinates Network, Circular Service, No. 21493, #1 (2017b), 21493
- The LIGO Scientific Collaboration the Virgo Collaboration 2017c, GRB Coordinates Network, Circular Service, No. 21934, #1 (2017c), 21934
- The LIGO Scientific Collaboration the Virgo Collaboration 2019, arXiv 1901.03310,